buildings

MDPI

Article

Employing Neural Networks, Fuzzy Logic, and Weibull Analysis for the Evaluation of Recycled Brick Powder in Concrete Compositions

Mohammad Mohtasham Moein [1,*], Komeil Rahmati [2], Ali Mohtasham Moein [3], Ashkan Saradar [2,*], Sam E. Rigby [4] and Amin Akhavan Tabassi [5]

1 Department of Civil Engineering, Allameh Mohaddes Nouri University, Nour 4641859558, Iran
2 Department of Civil Engineering, University of Guilan, Rasht 4199613776, Iran; komeil_rahmati@msc.guilan.ac.ir
3 School of Mechanical Engineering, Iran University of Science and Technology, Tehran 1684613114, Iran; ali.mohtasham.moein@gmail.com
4 Arup Resilience, Security & Risk, 3 Piccadilly Pl, Manchester M1 3BN, UK; sam.rigby@sheffield.ac.uk
5 Faculty of Business and Law, Manchester Metropolitan University, Manchester M15 6BX, UK; a.akhavan.tabassi@mmu.ac.uk
* Correspondence: m.mohtasham.moein@gmail.com (M.M.M.); ashkan.saradar@gmail.com (A.S.); Tel.: +98-911-182-5154 (A.M.M.)

Abstract: Using construction and demolition (C&D) waste in concrete production is a promising step toward environmental resilience amid the construction industry's ecological footprint. The extensive history of using bricks in the construction of buildings has resulted in a considerable amount of waste associated with this commonly used material. This study aimed to assess the quality of concrete by examining the effect of replacing cement with varying percentages of recycled brick powder (RBP—0% to 50%). The primary objectives include evaluating the mechanical properties of concrete and establishing the feasibility of using RBP as a partial cement substitute. The investigation of target concrete can be divided into two phases: (i) laboratory investigation, and (ii) numerical investigation. In the laboratory phase, the performance of concrete with RBP was assessed under short-term dynamic and various static loads. The drop-weight test recommended by the ACI 544 committee was used to assess the short-term dynamic behavior (352 concrete discs). Furthermore, the behavior under static load was analyzed through compressive, flexural, and tensile strength tests. During the numerical phase, artificial neural network models (ANN) and fuzzy logic models (FL) were used to predict the results of 28-day compressive strength. The impact life with different failure probabilities was predicted based on the impact resistance results, by combining the Weibull distribution model. Additionally, an impact damage evolution equation was presented for mixtures containing RBP. The results show that the use of RBP up to 15% caused a slight decrease in compressive, flexural, and tensile strength (about 3–5%). Also, by replacing RBP up to 15%, the first crack strength decreased by 7.15% and the failure strength decreased by 6.46%. The average error for predicting 28-day compressive strength by FL and ANN models was recorded as 4.66% and 0.87%, respectively. In addition, the results indicate that the impact data follow the two-parameter Weibull distribution, and the R^2 value for different mixtures was higher than 0.9275. The findings suggest that incorporating RBP in concrete can contribute to sustainable construction practices by reducing the reliance on cement and utilizing waste materials. This approach not only addresses environmental concerns but also enhances the quality assessment of concrete, offering potential cost savings and resource efficiency for the construction industry. Real-world applications include using RBP-enhanced concrete in non-structural elements, such as pavements, walkways, and landscaping features, where high strength is not the primary requirement.

Keywords: construction and demolition wastes; brick powder; impact strength; artificial neural networks; fuzzy logic; weibull distribution

check for updates

Citation: Mohtasham Moein, M.; Rahmati, K.; Mohtasham Moein, A.; Saradar, A.; Rigby, S.E.; Akhavan Tabassi, A. Employing Neural Networks, Fuzzy Logic, and Weibull Analysis for the Evaluation of Recycled Brick Powder in Concrete Compositions. *Buildings* **2024**, *14*, 4062. https://doi.org/10.3390/buildings14124062

Academic Editors: Yun Gao, Mohammad Hajmohammadian Baghban and Davoud Tavakoli

Received: 6 November 2024
Revised: 13 December 2024
Accepted: 20 December 2024
Published: 21 December 2024

Copyright: © 2024 by the authors. Licensee MDPI, Basel, Switzerland. This article is an open access article distributed under the terms and conditions of the Creative Commons Attribution (CC BY) license (https://creativecommons.org/licenses/by/4.0/).

1. Introduction

Since the onset of the 21st century, there has been a persistent escalation in global greenhouse gas (GHG) emissions, surpassing the levels observed from 1970 to 2000 [1–3]. Analyses of documents released by global organizations concerning planetary contamination consistently highlight the construction sector's role in exacerbating the environmental pollution crisis [4–7]. The production of concrete in the construction industry significantly contributes to the exacerbation of environmental pollution due to its high carbon footprint and resource-intensive processes [8,9]. The construction industry consumes approximately 40 billion tons of natural materials annually [8,10]. The extraction and processing of these materials lead to considerable environmental damage [8]. Within construction materials, cement stands out as a significant environmental challenge, responsible for emitting between 5% and 8% of global CO_2 emissions [11–15].

Mitigating the environmental impact of cement production by substituting a portion with viable alternatives presents a promising strategy for reducing planetary harm. Construction and demolition (C&D) waste offers a potential solution to this challenge. Specifically, recycled brick powder (RBP) emerges as an innovative alternative that can simultaneously address waste management and cement production environmental concerns. C&D waste encompasses materials such as bricks, concrete, ceramics, tiles, glass, plastics, and wood, among others [10,12,16]. Data indicate that China, the European Union, and the United States annually produce approximately 1800, 800, and 700 million tons of C&D waste, respectively [17,18]. Notably, these nations also lead in GHG emissions, collectively contributing to 47.1% of the global total—China at 29.2%, the United States at 11.2%, and the European Union at 6.7% [1]. Ultimately, C&D wastes are often relegated to disposal and landfilling [12].

Brick has been a staple in construction for centuries; however, the current demand for more efficient edifices has accelerated the cycle of demolition and reconstruction, consequently escalating the accumulation of brick waste. Recycled brick demonstrates promising potential as an alternative aggregate due to several key characteristics: (i) Its damaged state enhances pozzolanic activity, making it desirable as a cement substitute [19,20], (ii) Numerous studies have explored its microstructural properties [21,22], mechanical characteristics [23,24], and durability aspects [25,26]. Previous research has provided insights into the potential of recycled brick powder in concrete compositions: (i) Zheng et al. [27] found that 10% brick powder with specific particle sizes could exhibit comparable or superior mechanical attributes to benchmark specimens, (ii) Yang et al. [23] observed compressive strength improvements with less than 15% replacement, and (iii) Liu et al. [28] noted compressive strength improvements with 10% recycled brick addition.

Despite these promising findings, a critical gap remains in understanding the material's behavior under impact loading. Impact resistance is a crucial and intrinsic property of concrete within the realm of civil engineering applications [29,30], and is broadly defined as the capacity of concrete to absorb energy and maintain satisfactory dynamic behavior [31,32]. The susceptibility of various concrete structures—including wall panels, industrial flooring, bridge decks, and pavement systems for highways and airports—to impact loading presents a significant design challenge [33,34]. It necessitates the adoption of more sophisticated engineering designs aimed at enhancing impact resistance and augmenting the load-bearing capabilities of these elements [35,36]. Structural integrity can be compromised under various impact scenarios, including (i) Projectile collisions with concrete structures [37,38], (ii) Hydraulic shock from water impact [39], and (iii)Vehicular impact forces on concrete components [38,40]. The evaluation of impact resistance in concrete is conducted via diverse methodologies [34,41], with the repeated drop weight impact (RDWI) test considered the most common and cost-efficient [34,38]. Researchers have emphasized that the dispersion of data obtained from this test is significant [34,38], attributed to the test's inherent nature and the non-homogeneous conditions of concrete [34,42,43].

Critically, while numerous studies have examined various concrete characteristics incorporating brick powder, the behavior of this specific type of concrete under impact

loads remains unexplored. How does incorporating RBP as a partial cement replacement in concrete impact the impact resistance of structures while addressing environmental issues related to C&D waste and greenhouse gas emissions? This study seeks to clarify this question and contribute to the field by systematically investigating concrete mixtures with varying percentages of recycled brick powder (5%, 10%, 15%, 20%, 25%, 30%, 35%, 40%, 45%, and 50%) and comprehensively evaluating their compressive, tensile, flexural, and impact strength characteristics.

1.1. Research Background

Given the significance of sustainable development, researchers have assessed diverse facets of cement composites incorporating RBP in recent years. Zheng et al. [27] analyzed mortar specimens integrated with varying proportions (10%, 20%, and 30%) of clay brick powder characterized by particle sizes (0.3 mm, 0.1 mm, 0.06 mm, and 0.04 mm). The findings indicated that specimens comprising 10% brick powder with particle sizes of 0.1 and 0.06 mm exhibited comparable or superior mechanical attributes relative to the benchmark specimen. Furthermore, it was observed that an escalation in both the replacement ratio and the mean particle diameter corresponded with a reduction in compressive strength. Yang et al. [23] evaluated the foam concrete by different percentages of RB. In this regard, the improvement of compressive strength was concluded for less than 15% replacement, but when more than 30% RB was used in the mixture, the compressive strength decreased drastically. The investigation further revealed that the effect of RB content on the compressive strength was more pronounced in low-density foam concrete compared to its high-density counterpart. Liu et al. [28] concluded that the compressive strength of mortar is improved with the addition of 10% RB. Further, they noted that the energy consumption for grinding clay brick into powder is lower than that for aerated concrete blocks. Zhu et al. [44] explored the substitution of RB for silica fume and cement within the matrix of reactive powder concrete (RPC). Incremental replacement of cement with RB yielded the following outcomes: (i) a marginal reduction in flowability, (ii) a slight alteration in compressive strength, (iii) a reduction in flexural strength, (iv) a decrease in shrinkage, and (v) diminished resistance to chloride penetration. Similarly, elevating the proportion of RB instead of silica fume led to (i) a minor decline in flow, (ii) a tendency for reduced compressive and flexural strength, (iii) lessened shrinkage, and (iv) lowered chloride ingress resistance. Likes et al. [45] examined the use of eco-friendly recycled powders (RPs), specifically recycled concrete powder (RCP) and recycled brick powder (RBP), as supplementary cementitious materials in concrete to reduce cement demand and CO_2 emissions. Although the RPs demonstrated lower pozzolanic activity compared to conventional materials, they achieved strength activity indexes exceeding 75% and enhanced durability, particularly with RBP, which improved surface resistivity by 24%. The study concludes that RPs can positively influence the properties of concrete; however, their limited pozzolanic activity may restrict broader applications. Wu et al. [26] examined the effects of incorporating recycled brick aggregate and its powder into a cement matrix. Their research indicated that RB powder could diminish the quantity of hydration products within cement-based materials, with a notable reduction manifesting at a 50% substitution rate. The presence of RB powder was found to curtail fluidity and prolong the setting duration of cementitious compositions. The study also noted that an extensive inclusion of RB amplified drying shrinkage, whereas the introduction of RB powder mitigated this effect, suggesting a 30% replacement level as optimal. Consequently, a mortar blend containing 50% RB aggregate and 30% RB powder demonstrated reduced drying shrinkage compared to mixtures devoid of RB constituents. Table 1 presents a comprehensive report on the impact of varying percentages of brick powder on the mechanical properties, durability, and microstructure of cement composites.

Table 1. Summary of studies on RBP.

N.O.	Characteristic		Recommended Dosages and Effects	Ref.
1	Mechanical properties	Compressive strength	[15%] (28 days) = 16.36% ↓ [30%] (28 days) = 22.58% ↓ [45%] (28 days) = 34.80% ↓	[46]
2			[10%] (28 days) = 1.012% ↑ [30%] (28 days) = 17.35% ↓ [50%] (28 days) = 25.34% ↓	[26]
3			[10%] (28 days) = 1.763% ↑ [30%] (28 days) = 3.007% ↓ [50%] (28 days) = 5.656% ↓	[47]
4		Flexural strength	[5%] (28 days) = 3.863% ↓ [10%] (28 days) = 7.726% ↓ [15%] (28 days) = 0.000% ↓	[48]
5			[10%] (28 days) = 1.531% ↓ [30%] (28 days) = 2.735% ↓ [50%] (28 days) = 4.814% ↓	[49]
6			[10%] (28 days) = 5.165% ↓ [20%] (28 days) = 9.289% ↓ [30%] (28 days) = 27.61% ↓	[47]
7		Tensile strength	[10%] (28 days) = 6.432% ↓ [30%] (28 days) = 4.970% ↓ [50%] (28 days) = 13.45% ↓	[49]
8			[10%] (28 days) = 3.530% ↓ [20%] (28 days) = 11.95% ↓ [30%] (28 days) = 26.15% ↓ [40%] (28 days) = 33.14% ↓	[50]
9		Impact strength	Examining exclusively brick powder instead of cement = Research gap	---
10	Durability performance	Chloride diffusivity	[5%] = 1.067% ↓ [25%] = 1.779% ↓ [30%] = 80.42% ↑	[25]
11			[20%] = 30.95% ↓ [30%] = 42.85% ↓ [40%] = 38.09% ↓	[51]
12			[10%] = 24.08% ↓ [30%] = 68.70% ↓ [50%] = 85.00% ↓	[26]
13	Microstructure		The products of cement paste hydration by RB mainly consist of C-S-H gel, ettringite, and $Ca(OH)_2$, laying the foundation for the creation of a more compact structure.	[46]
14			The interfacial transition zone (ITZ) between the RB particle and cement hydration products is compact with no apparent loose material in this area.	[28]

The ↓ symbol indicates a decrease, and the ↑ symbol indicates an increase.

1.2. Artificial Neural Networks (ANN), Fuzzy Logic (FL), and Weibull Distribution

The assessment of concrete properties in the laboratory invariably involves both time and financial costs. This complexity is further compounded by the introduction of human errors and variations in laboratory conditions, in addition to the inherent factors of time and cost. Consequently, a reliable estimation of the target concrete's properties offers a viable solution to address the uncertainty associated with laboratory results [52–55]. In recent years, researchers have shown interest in employing artificial neural network (ANN)

methods and fuzzy logic (FL) for predicting concrete's mechanical characteristics [56–58], as well as utilizing the Weibull distribution to assess concrete behavior under short-term dynamic loads [34,59].

ANNs constitute a subset of machine learning models inspired by the organization of neurons in living organisms. ANNs find crucial applications in signal reception, processing, and transmission within the field of artificial intelligence [60–62]. The architecture of an ANN comprises three layers [63,64]: the input layer (which houses input parameters for training and testing), the hidden layer/s (facilitating communication between the input and output layers), and the output layer (responsible for producing results). The study of Mohtsham Moin et al. [65] provides a complete review of the use of this algorithm in concrete technology. Askarzadeh was the first to introduce the concept of fuzzy sets [66]. FL has proven instrumental in addressing various decision-making challenges, often yielding optimal decisions based on input data. Rooted in human decision-making processes, FL can be seen as an evolution of Aristotle's Logic or Boolean Logic [67–69]. In contemporary applications, FL has given rise to concepts such as fuzzy numbers, fuzzy arithmetic, and statistical tools like fuzzy clustering. Notably, devices and computers designed around FL outperform their counterparts relying solely on Boolean logic. This theory operates based on "if-then" rules, facilitating understanding of the relationships between input and output variables [70,71]. Researchers have explored the use of FL for evaluating concrete properties [72,73]. The Weibull distribution model [74] emerged from the study of material fatigue life. In industrial contexts, the Weibull distribution finds widespread application for predicting the lifespan of brittle materials. Beyond industry, various other fields leverage the Weibull distribution to analyze rainfall patterns in hydrology, study the lifespan of organisms in biology, and model stock market behavior in finance. The effectiveness of the Weibull distribution has been underscored by Jung and Schindler [75] in a comprehensive review of 46 studies conducted between 2010 and 2018. Additionally, other researchers have highlighted the practical applicability of this distribution in both research and industry [76–79]. Notably, in recent years, there has been significant interest in utilizing the Weibull distribution to analyze the behavior of concrete under short-term dynamic loads, with positive feedback regarding the performance of this distribution model [12,80–82].

1.3. Significance of the Research

The construction industry is a major contributor to global greenhouse gas (GHG) emissions, with the cement manufacturing process being a significant source. Utilizing waste materials, such as RBP, as a partial replacement for cement can help mitigate the environmental impact of concrete production. This study aims to investigate the performance of concrete mixtures containing varying percentages of RBP (5–50%) under both static (compressive, tensile, and flexural) and short-term dynamic (impact) loading conditions. Previous research on RBP-based concrete has been limited in scope, focusing on a narrow range of RBP substitutions. This work expands the understanding of RBP-concrete behavior by systematically evaluating a wider range of replacement levels.

Moreover, this study employs advanced predictive models, such as ANN and FL, to estimate the compressive strength of the concrete mixtures. This approach provides valuable insights into the applicability of these models for predicting the performance of RBP-based concrete. Lastly, the investigation of RBP-concrete's response to short-term dynamic loads, such as impact, addresses a notable research gap in the existing literature. The use of the two-parameter Weibull distribution to analyze the impact test results offers a practical approach for industry application.

Overall, this research contributes to the development of more sustainable concrete materials, which can help the construction industry reduce its environmental footprint and achieve the global net-zero emissions targets. Figure 1 shows an overview of the process of different stages of this study.

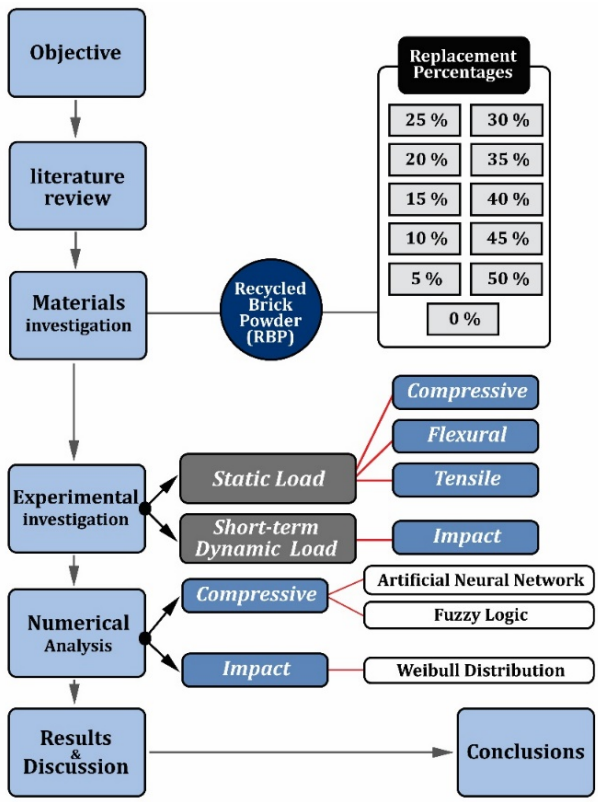

Figure 1. Methodology.

2. Experimental Program

2.1. Materials

The materials employed in this study comprised cement, superplasticizer, aggregates, water, and brick powder. Specifically, Type II cement, as detailed in Table 2, was utilized. The consumable superplasticizer belongs to the third generation, and its technical specifications are outlined in Table 3. The aggregates employed are of river origin. Coarse and fine aggregates exhibit standard grading within the range of 4.75–19 mm and 0–4.75 mm, respectively. Table 4 presents the aggregate grading according to ASTM C33 [83] standards. According to previous studies [20,23,84,85], four stages of preparation were undertaken to obtain the desired brick powder. Figure 2 presents a report detailing the steps taken to achieve the target brick powder. The waste bricks used in this study were collected from building demolition sites in Rasht, Iran. Table 5 provides information on the chemical characteristics of the utilized brick powder. Brick powder used in this study is shown in Figure 3.

Table 2. Chemical and physical characteristics of the cement.

Chemical Properties		Physical Properties		
SiO_2	21.27	Compressive strength (kgf/cm^2)	3 days	205
Al_2O_3	4.95		7 days	288
Fe_2O_3	4.03		28 days	411
CaO	62.95	Setting time	Initial	154
MgO	1.55		Final	195
SO_3	2.26	Longitudinal expansion		1.5 mm—0.08%
Na_2O	0.49			
K_2O	0.65	Special surface (cm^2/gr)		2910
C_3A	6.30			

Table 3. Specifications of superplasticizer.

Technical Features	
Generation	3
Physical State	Liquid
Color	Opaque green
Specific weight	1.2 ± 0.02 kg/lit
Chlorides (PPM)	500 max
Chemical Base	Modified polycarboxylate ether

Table 4. Grading of aggregates.

Fine		Coarse		Sieve Size
This Study	ASTM C33 [83]	This Study	ASTM C33 [83]	
100	---	100	100	25 mm
100	---	92	90–100	19 mm
100	100	50.12	20–55	9.5 mm
99.94	95–100	6.558	0–10	4.75 mm
92.67	80–100	0.262	0–5	2.36 mm
74.23	50–85	---	---	1.18 mm
53.51	25–60	---	---	600 mm
20.43	10–30	---	---	300 mm
3.61	2–10	---	---	150 mm

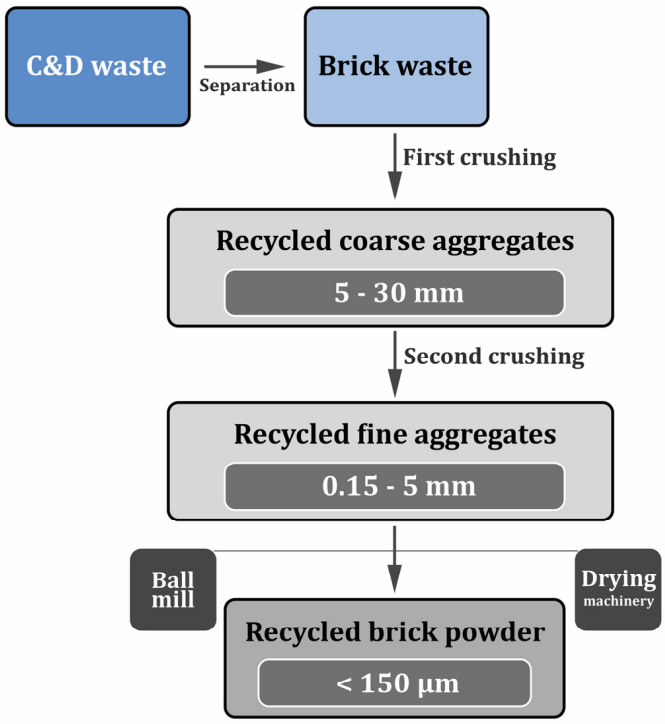

Figure 2. Brick powder production process.

Table 5. Chemical characteristics of brick powder.

Chemical Properties												
L.O.I.	Fe_2O_3	CaO	SO_3	TiO_2	P_2O_5	K_2O	MnO	SiO_2	Na_2O	MgO	Al_2O_3	Ref.
0.73	7.36	2.02	0.929	0.43	0.194	1.05	0.072	60.43	1.04	3.04	12.79	This study
0.42	8.26	17.29	0.34	---	0.11	1.19	0.18	30.82	0.02	3.37	13.17	[86]
---	4.8	1.3	---	---	---	---	---	76.1	---	1.7	11.8	[26]
---	5.15	46.78	---	---	---	2.77	---	53.8	0.65	2.58	13.2	[44]
ASTM C618 [87]												
This Study			Permissible range					Parameter				
80.58			>70					SiO_2 +Al_2O_3 +Fe_2O_3				
0.929			<0.3					SO_3				
0.73			<10					L.O.I.				
0.12			<0.8					Autoclave expansion				
0.5			<3.0					Moisture content				

Figure 3. Brick powder.

2.2. Mix Designs

Eleven mixed designs were explored, with details regarding the composition of each mixed design presented in Table 6. Mixture 1, designated as the control group, contained no brick powder and served as a baseline to evaluate the performance of mixtures incorporating brick powder. Mixtures containing brick powder were designated as "RBx", where "x" represents the percentage of cement replaced with brick powder. For instance, RB5 denotes a mixture with 5% brick powder replacing cement, and RB10 signifies a mixture containing 10% brick powder. The incorporation of brick powder as a cement substitute progressed in increments of 5%, culminating in the RB50 mixture, which comprised the maximum replacement level of 50%. A water-to-cement ratio of 0.4 was maintained for all mixtures.

2.3. Sample Preparation

The preparation of different materials was conducted in this study following ASTM C192 [88] and the technical points of previous studies [20,49,89] were also considered. Initially, fine and coarse aggregates were introduced into the mixer, along with half of the required water, and mixed for 30 s. Subsequently, cement and brick powder were incorporated into the mixer, and the mixing process continued for another 30 s. Finally, the superplasticizer and the remaining half of the water were added, and the mixing was extended for an additional 3 min. Fresh concrete mixtures were cast into molds (cubic, prism, and cylindrical). Following molding, the samples were shielded with plastic covers for approximately 24 h to prevent surface water evaporation. Subsequently, the samples

were extracted from the molds and subjected to curing in a water basin at a temperature of 23 ± 1 °C until they reached the desired test age.

Table 6. Mix design (kg/m^3).

Mix No.	Mix Code	Cement	Brick Powder	Water	Aggregates		SP
					Fine	Coarse	
1	Control	400	0	160	848.91	1021.90	1.2
2	RB5	380	20	160	397.00	1594.90	1.6
3	RB10	360	40	160	397.84	1598.26	2
4	RB15	340	60	160	398.89	1602.48	2
5	RB20	320	80	160	399.51	1604.99	2.8
6	RB25	300	100	160	400.56	1609.20	2.8
7	RB30	280	120	160	401.40	1612.57	3.2
8	RB35	260	140	160	402.23	1615.93	3.6
9	RB40	240	160	160	403.28	1620.14	3.6
10	RB45	220	180	160	404.12	1623.50	4
11	RB50	200	200	160	404.96	1626.87	4.4

2.4. Test Methods

This study investigated the mechanical behavior of concrete under various loading conditions, including static compressive, flexural, and tensile loads, as well as short-term dynamic impact loads. Details regarding the specific tests and sample specifications are presented in Table 7.

Table 7. Description of tests and details.

Shape		Number of Samples	Dimension (cm)			Curing	Standard	Test	N.O.
			c	b	a				
	Cube	33	15	15	15	28	BS EN 12390-3 [90]	Compressive strength	1
	Prism	33	4	4	16	28	ASTM C348 [91]	Flexural strength	2
	Cylinder	33	---	30	15	28	ASTM 496 [92]	Tensile strength	3
	Cylinder	88 (352 discs)	---	30	15	28	ACI 544 [93]	Impact strength	4

For compressive strength, testing was conducted following BS EN 12390-3 [90] at 28 days of curing on cubic specimens measuring 15 × 15 × 15 cm. Flexural strength was determined following ASTM C348 [91] at 28 days on prismatic specimens with dimensions of 16 × 4 × 4 cm. Tensile strength was evaluated according to ASTM C496 [92] at 28 days on cylindrical specimens measuring 15 × 30 cm. In accordance with ACI 544 [93] recommendations, the RDWI test was employed to investigate the impact behavior of the target concrete. Cylindrical samples (15 cm diameter × 30 cm height) were sectioned into four discs with a diameter of 15 cm and a thickness of 6.4 cm for this purpose. A total of 32 concrete discs (8 cylindrical samples per mixture) were subjected to the RDWI test. Figure 4 presents a report on the number of samples and concrete discs for the RDWI test. Figures 5 and 6 display the RDWI testing apparatus and the specifications of its various

components. During the RDWI test, various parameters were recorded, including the first crack strength, failure strength, increase in the number of post-first crack blows (INPB), energy absorption (E), and Impact Ductility Index (IDI). The first crack strength represents the number of blows required to induce an initial crack in the concrete disc. Similarly, the failure strength corresponds to the number of blows necessary to cause contact with three out of the four metal lugs surrounding the disc. The INPB parameter is calculated by subtracting the number of blows for first crack resistance from the number of blows for failure resistance. Equations (1) and (2) will detail the calculation of the IDI and impact energy E.

$$IDI = (N_{failure} - N_{first})/N_{first} \tag{1}$$

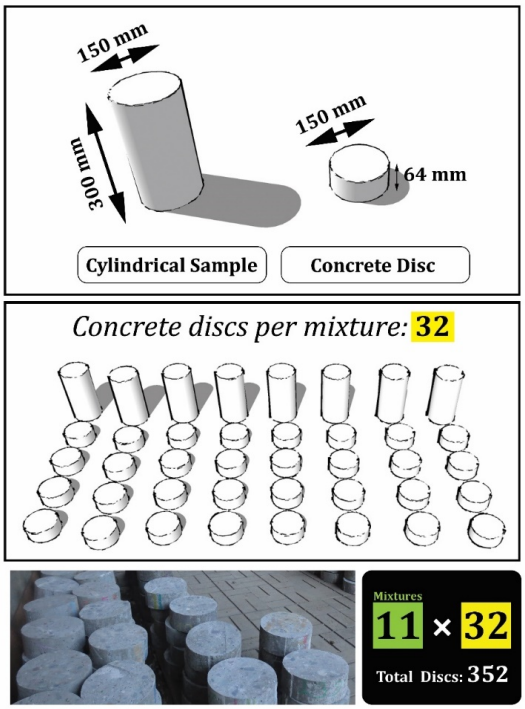

Figure 4. Number of samples and concrete discs in the RDWI test.

Figure 5. RDWI test device.

$$E = mgh \tag{2}$$

In Equations (1) and (2): *IDI*—impact ductility index, N_{first}—First visual crack, $N_{failure}$—ultimate crack, *E*—impact energy (J), *m*—mass of hammer, *g*—gravitation acceleration, and *h*—height of drop.

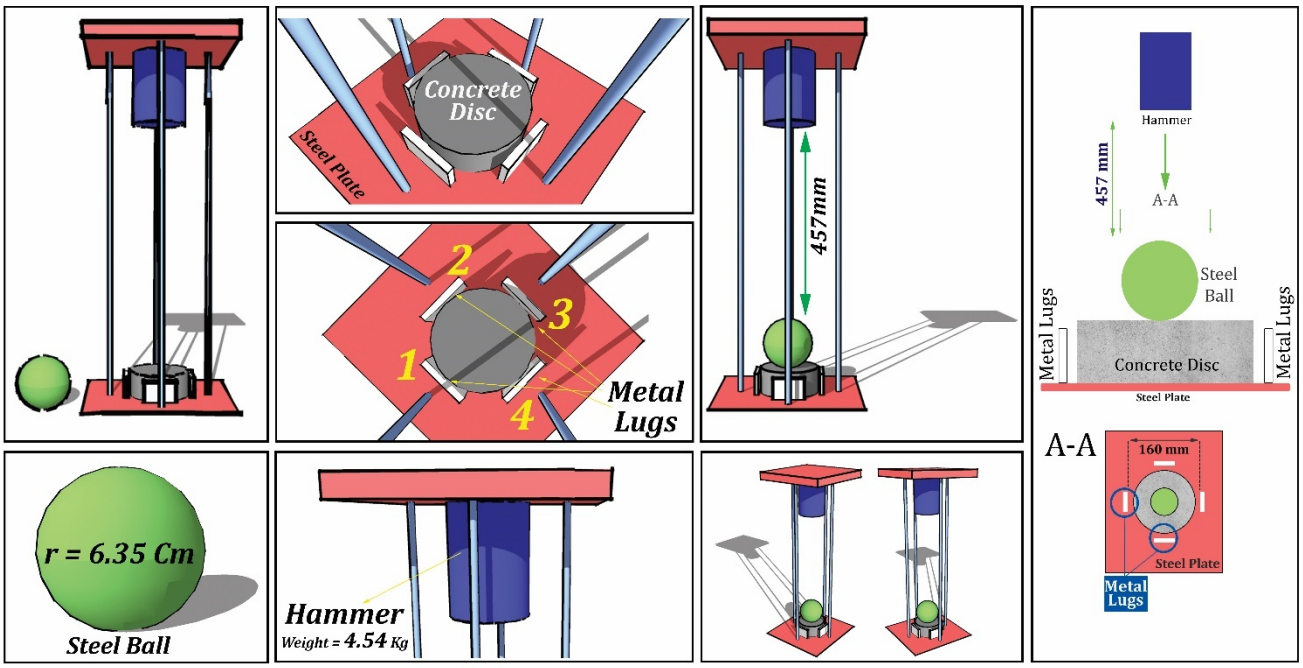

Figure 6. Specifications and details of the RDWI test device.

3. Prediction Models

This study used input variables such as cement, brick powder, and Superplasticizer. Table 8 shows the characteristics of these variables. An ANN with a forward multi-layer perceptron structure and a backpropagation training algorithm with the Levenberg–Marquardt optimization method was employed. The Levenberg–Marquardt algorithm can randomly divide the input and output vectors of the network into three sets, including training, validation, and test data. Mean squared error (MSE) was used as a stopping measure for the network (Equation (3)). The R-value, indicating the relationship between network output and real values, was considered (Equation (4)).

$$MSE = \frac{\sum_{j=0}^{P} \sum_{i=0}^{N} \left(d_{ij} - y_{ij}\right)^2}{N \times P} \tag{3}$$

$$R^2 = 1 - \frac{\sum_{i=1}^{N} (y_i - \hat{y}_i)^2}{\sum_{i=1}^{N} (y_i - \tilde{y}_i)^2} \tag{4}$$

Table 8. Characteristics of the input and output variables.

Statistical Characteristic	Input			Output
	Cement	Brick Powder	Superplasticizer	Compressive Strength
Min.	200	0	1.2	36.13
Max.	400	200	4.4	52.80
Mean.	300	100	2.836	45.86
SD.	66.3	66.3	1.035	5.85

In Equations (3) and (4): N is the number of predictions, p is the number of processed output elements, y_{ij} is the network output for sample i in processed element j, and d_{ij} is the desired output of the network for sample i in processed element j. Additionally, y represents the actual values, $\hat{y}$ represents the predicted values, and $\tilde{y}$ represents the average values. In this study, two neurons in the hidden layer were chosen to predict the 28-day compressive strength. Hence, the neural network's configuration is 3-2-1: 3 inputs, 2 hidden layer neurons, and 1 output. The general structure of the ANN model employed in this study is illustrated in Figure 7a.

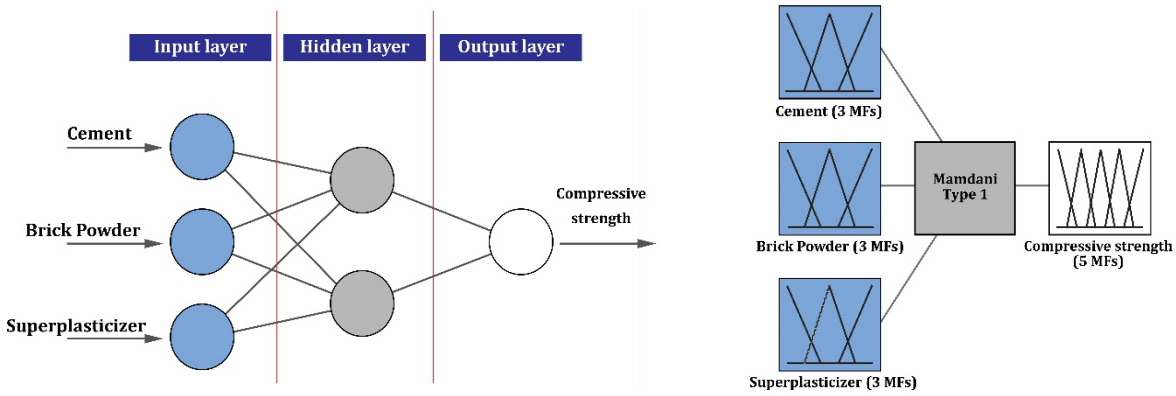

(**a**) (**b**)

Figure 7. 28-day compressive strength prediction models: (**a**) Artificial Neural Network (ANN); (**b**) Fuzzy Logic (FL).

The FL model with three input variables was developed to predict compressive strength values (28 days). MATLAB R2022a was used to utilize the FL model for this prediction. Prediction was based on rules expressed in IF-Then form. Fuzzy sets were used in Mamdani's inference system [94–96] for the output, resulting in non-linear and fuzzy output for each rule. Triangular membership functions based on experience were constructed for fuzzy logic as shown in Figure 7b.

4. Discussion and Results

This section presents a comprehensive analysis of the experimental findings and their implications for the use of brick powder in concrete. The discussion integrates the results obtained from various tests, including compressive, flexural, tensile, and impact strength, with a focus on understanding the impact of substituting cement with brick powder. The subsequent sections delve into specific aspects of the experimental investigation, providing insights into how these findings align with or diverge from existing literature. The results of the experiments were analyzed using the ANN model, FL model, and a two-parameter Weibull distribution. This approach aims to elucidate the practical significance of the research and its contribution to the field of sustainable construction materials.

4.1. Experimental Investigation

4.1.1. Compressive Strength

The experimental investigation of compressive strength is crucial for understanding the impact of brick powder on concrete's performance. Figure 8 illustrates the compressive strength outcomes for various mixtures incorporating differential ratios of brick powder. The control mixture manifested a compressive strength of 52.8 MPa at 28 days. The partial replacement of cement with brick powder precipitated a diminution in compressive strength at 28 days. A mixture with a 5% brick powder composition (RB5) exhibited compressive strength nearly commensurate with the control, registering 52.1 MPa. Mixtures with 10% (RB10) and 20% (RB20) brick powder correspondingly demonstrated compressive

strengths of 51.3 MPa and 47.83 MPa, respectively. The decrease in compressive strength persisted across other mixtures until the mixture with 50% powdered brick (RB50) exhibited the lowest compressive strength at 36.134 MPa.

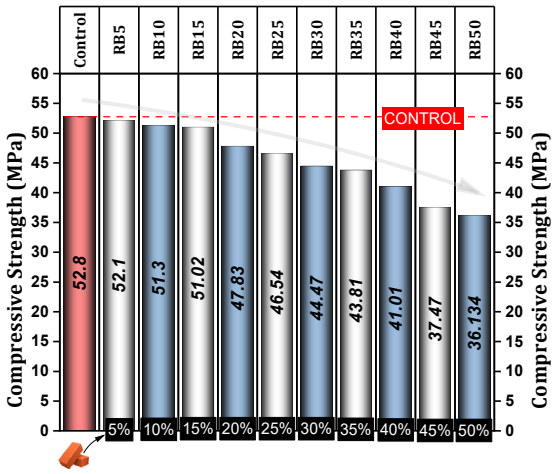

Figure 8. Average results of 28-day compressive strength.

Figure 9 illustrates the variation in compressive strength for mixtures containing brick powder compared to the control mixture. The overall reduction in compressive strength resulting from substituting brick powder for cement falls within the range of 1.33% to 31.57%. The strength reduction rates for RB5, RB10, and RB15 mixtures are 1.33%, 2.85%, and 3.38%, respectively, which closely aligns with the behavior of the control mixture. When substituting brick powder by more than 15%, a more pronounced reduction in strength is observed. Specifically, for mixtures containing 20% to 35% brick powder, the reduction in strength falls within the range of 9.42% to 17%. However, using 40% brick powder (RB40) results in a 20% decrease in resistance, and 50% brick powder leads to a reduction exceeding 30%. Reducing compressive strength by substituting brick powder for cement can result from several factors [20,97–102]: (i) cement content reduction, (ii) incomplete hydration, (iii) pore-induced stress concentration, (iv) interfacial transition zone (ITZ), and (v) water demand increase.

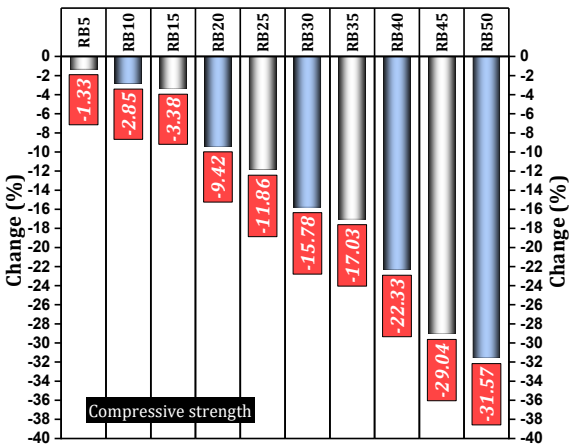

Figure 9. 28-day compressive strength changes compared to the control mix.

Figure 10 presents the compressive strength results from prior studies investigating the use of brick powder as a partial replacement for cement [23,26,27,46,47,103–106]. Results from various studies consistently indicate a negative correlation between the dosage of brick powder and its compressive strength, suggesting that increasing the dosage decreases the compressive strength. This trend was observed in six out of eight reviewed articles,

demonstrating a strong correlation. The studies by Lin et al. [103] and Karatas et al. [104] exhibited high R^2 values exceeding 0.94, indicating a suitable fit of the regression model to the data. Liu et al. [46] and Heidari et al. [105], with R^2 values of 0.9725 and 0.9797, respectively, achieved the best results in explaining variations in compressive strength. However, Yang et al. [23] revealed an anomalous trend with a positive regression coefficient, implying a potential shift like the dosage effect on compressive strength. The present study, employing a linear regression model ($y = -0.3464x + 54.521$) with an R^2 value of 0.9638, demonstrates a high level of accuracy in explaining the data. Compared to other findings, the slope coefficient in this research is within a reasonable range when averaged with previous studies and can serve as a starting point for optimizing dosage in practical applications.

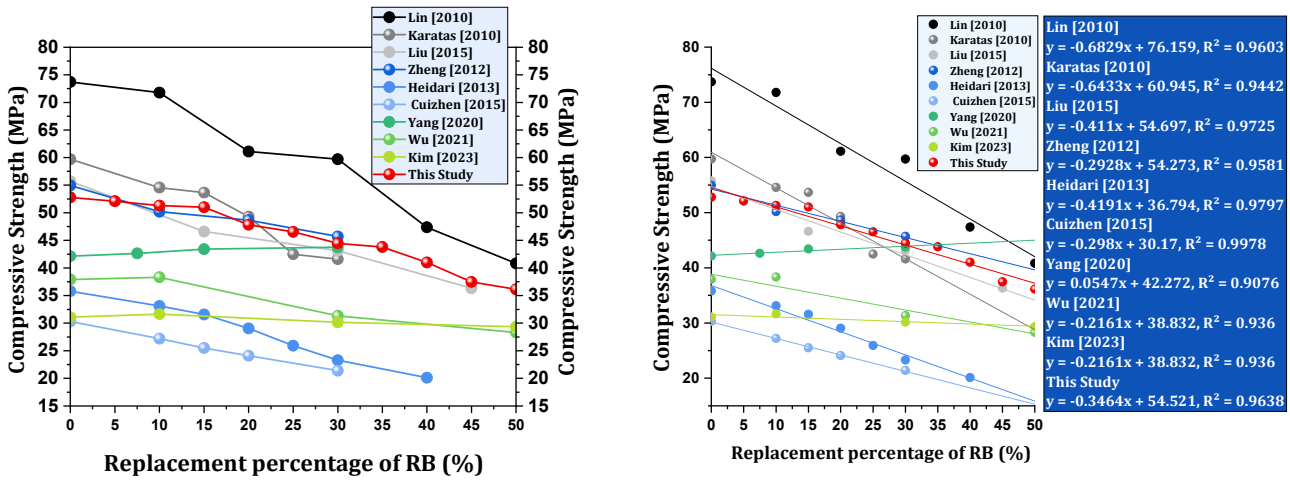

(**a**) (**b**)

Figure 10. Prior research on compressive strength [23,26,27,46,47,103–106]: (**a**) Impact of brick powder; (**b**) Regression analysis of compressive strength versus varying brick powder doses.

4.1.2. Flexural Strength

The flexural strength results of mixtures containing brick powder are presented in Figure 11. Among the various mixtures, the control mixture, with a flexural strength of 7.62 MPa, exhibits the highest strength. Notably, the mixture containing 5% brick powder (RB5) demonstrates the highest flexural strength, measuring 7.56 MPa. Additionally, the mixtures with 10% brick powder (RB10) and 15% brick powder (RB15) yield results of 7.49 MPa and 7.32 MPa, respectively. However, as the proportion of brick powder replacement increases, the trend shows a consistent decrease in flexural strength. Ultimately, the lowest flexural strength of 5.91 MPa is recorded for the mixture containing 50% brick powder (RB50).

Figure 12 illustrates the changes in flexural strength of mixtures containing different percentages of brick powder compared to the control mixture. The general range of flexural strength reduction resulting from various percentages of brick powder substitution ranges from 0.79% to 23%. Specifically, the BR5 mixture experiences a very small loss in flexural strength, approximately 0.79%. Similarly, the BR10 mixture exhibits a 1.71% drop in flexural strength, while the BR15 mixture shows a 3.94% reduction, indicating behavior close to that of the control mixture. However, when brick powder replacement exceeds 15%, the decrease in flexural strength becomes more pronounced. Notably, replacing 20% to 40% of brick powder results in a flexural strength reduction ranging from 8.27% to 18.77%. The most significant reduction occurs in the mixture containing 50% brick powder (RB50), with a 22.45% decrease. Brick powder, unlike cement, does not serve as a robust bonding agent. When it is substituted in place of cement, the overall structure weakens. Brick powder can absorb a portion of the mixed water required for hydration. Consequently, this reduces the

available water for cement hydration, potentially leading to an incomplete reaction and a weaker overall structure with reduced flexural strength. Additionally, brick powder can diminish the interlocking between particles, which may hinder the formation of a strong and coherent matrix within the concrete [20,97,98,107].

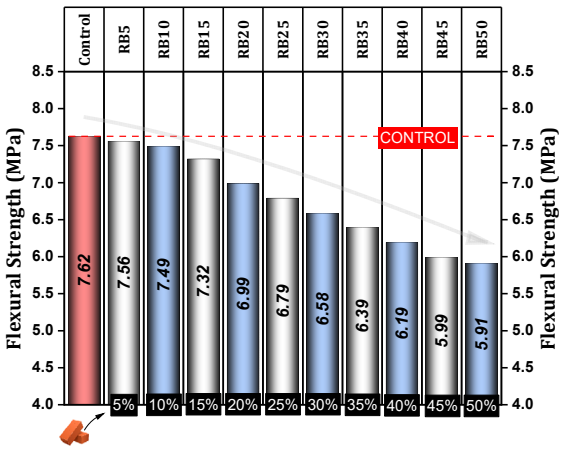

Figure 11. Average results of 28-day flexural strength.

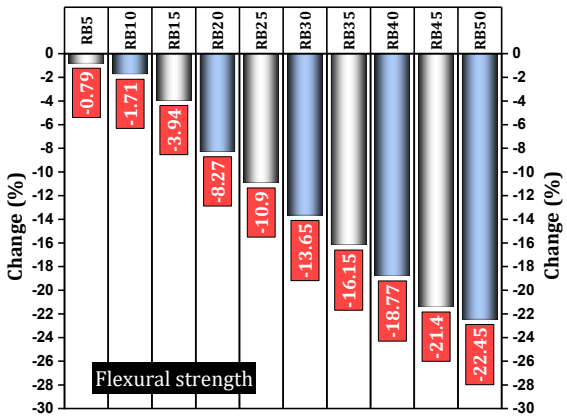

Figure 12. 28-day flexural strength changes compared to the control mix.

The flexural strength results from previous studies investigating the use of brick powder as a substitute for cement are presented in Figure 13. Analyzing different studies reveals two general trends related to flexural strength. The prevailing trend in most studies indicates a reduction in flexural strength when brick powder is used as a replacement, although this reduction is more insignificant for low replacement percentages. However, some studies have found that a small percentage (approximately 5–10%) of brick powder increases flexural strength; a phenomenon likely attributed to improved packing density. Based on the regression analysis results from various studies, several key points can be highlighted in comparison to the present study. Initially, the studies by Zheng et al. [27] and Ge et al. [89] demonstrated a strong correlation between flexural strength and brick powder dosage, with R^2 values of 0.90 and 0.9792, respectively, indicating that variations in powder dosage significantly affect flexural strength. This suggests that increasing the powder dosage may not directly lead to a substantial increase in flexural strength, as both studies observed a negative relationship between the two variables. In contrast, the studies by Ortega et al. [108], Letelier et al. [48], and Rani et al. [102] exhibited a weaker regression relationship. Specifically, the results of the present study, with an R^2 value of 0.9852, indicate a strong and significant correlation between brick powder dosage and flexural strength. This study shows that increasing the powder dosage significantly influences flexural strength, although the slope is negative, meaning that as the dosage increases,

flexural strength gradually decreases. However, the high R^2 value indicates the robustness of the regression model. This analysis reveals that while some studies show conflicting results, the present study clearly demonstrates a significant impact of brick powder dosage on flexural strength. This finding can contribute to the design and optimization of the use of brick powder in construction materials.

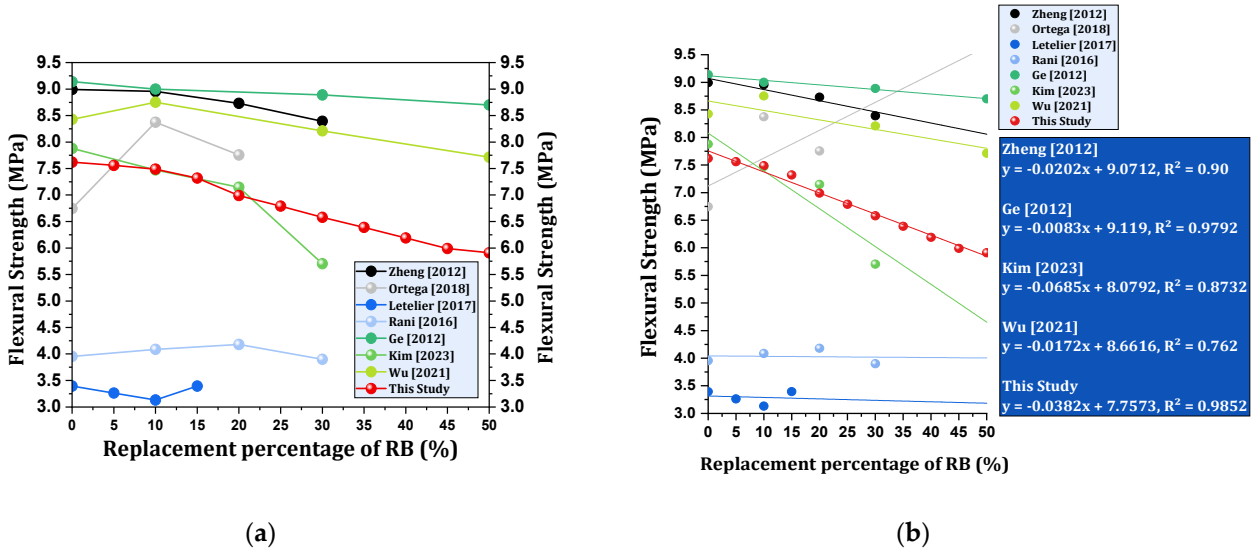

(**a**) (**b**)

Figure 13. Prior research on flexural strength [26,27,47–49,89,102,108]: (**a**) Impact of brick powder; (**b**) Regression analysis of flexural strength versus varying brick powder doses.

4.1.3. Comparative Analysis of Compressive and Flexural Strength Changes

Figure 14 presents a comparison of the changes in compressive and flexural strength resulting from different replacement percentages of the brick powder compared to the control mixture. Notably, the decrease in compressive strength is more pronounced than that in flexural strength. Additionally, the impact of low brick powder replacement percentages exhibits minimal intensity. Moving on to Figure 15, it highlights the magnitude of the reduction in compressive and flexural strength observed in studies conducted by Zheng et al. [27] and Wu et al. [26]. In this context, it becomes evident that the severity of the decrease in compressive strength surpasses that in flexural strength.

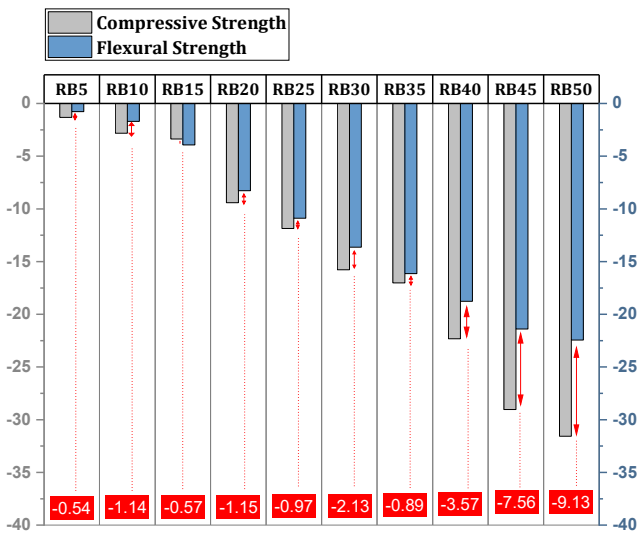

Figure 14. The intensity of changes in compressive and flexural strength.

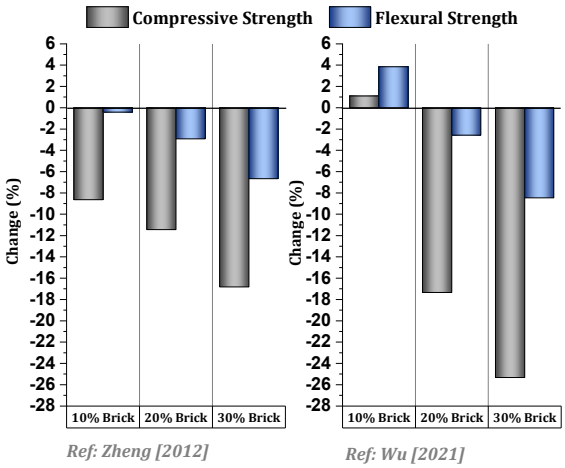

Figure 15. Examining the severity of changes in compressive and flexural strength in previous studies [26,27].

4.1.4. Tensile Strength

The tensile strength results of mixtures containing different percentages of brick powder and their changes compared to the control mixture are shown in Figure 16. The control mixture achieved a tensile strength of 2.2 MPa, outperforming other mixtures. Substituting brick powder by 5%, 10%, and 15% resulted in decreases of 2.15%, 4.05%, and 5.48%, respectively. Interestingly, replacing 20% brick powder caused a decrease in tensile strength. Furthermore, when brick powder was replaced by 30%, the tensile strength decreased by more than 20%. This decreasing trend persisted until the weakest performance was recorded for RB45 and RB50 mixtures, with reductions of 38.1% and 40.96%, respectively. Figure 17 illustrates the trend of tensile strength results influenced by brick powder replacement in other studies [49,50,101,102]. While limited research has explored the tensile strength of concrete containing brick powder as a cement substitute, the findings indicate that at low dosages of brick powder, there is a decreasing trend in tensile strength. Interestingly, some cases even report a slight increase in resistance. However, when brick powder replacement is high, the trend shifts toward a decrease in tensile strength. This study analyzes and compares the results of regression analysis between tensile strength and brick powder dosage. Results from four other studies are also presented to provide a better understanding of the relationship between dosage and tensile strength. Specifically: The study by Nepomuceno et al. [49] has a regression equation of $y = -0.0076x + 3.378$ with a coefficient of determination $R^2 = 0.7819$, indicating a relatively weak correlation between dosage and tensile strength. The study by Rani et al. [102] has a stronger correlation, with an equation of $y = -0.0497x + 12.251$ and $R^2 = 0.8512$, suggesting a significant impact of dosage on tensile strength. The studies by Kim et al. [101] and Olofinnade et al. [50] also indicate very strong correlations between dosage and tensile strength, with equations $y = -0.0327x + 3.86$ and $y = -0.0335x + 3.8783$, and R^2 values of 0.978 and 0.9648, respectively. Finally, the results of our study show that the regression equation $y = -0.0357x + 4.3591$ with $R^2 = 0.969$ demonstrates a significantly stronger correlation with brick powder dosage and provides a more accurate conclusion compared to other studies. These findings suggest that increasing the dosage of brick powder has a significant negative impact on tensile strength, which is consistent with the results of other studies.

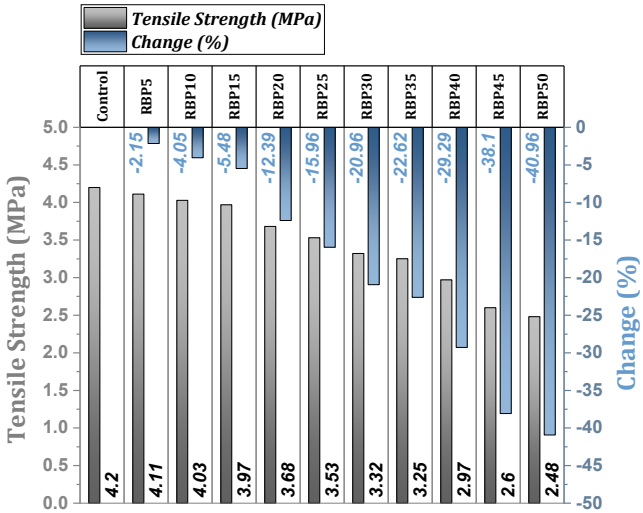

Figure 16. Average 28-day tensile strength results and changes compared to the control mixture.

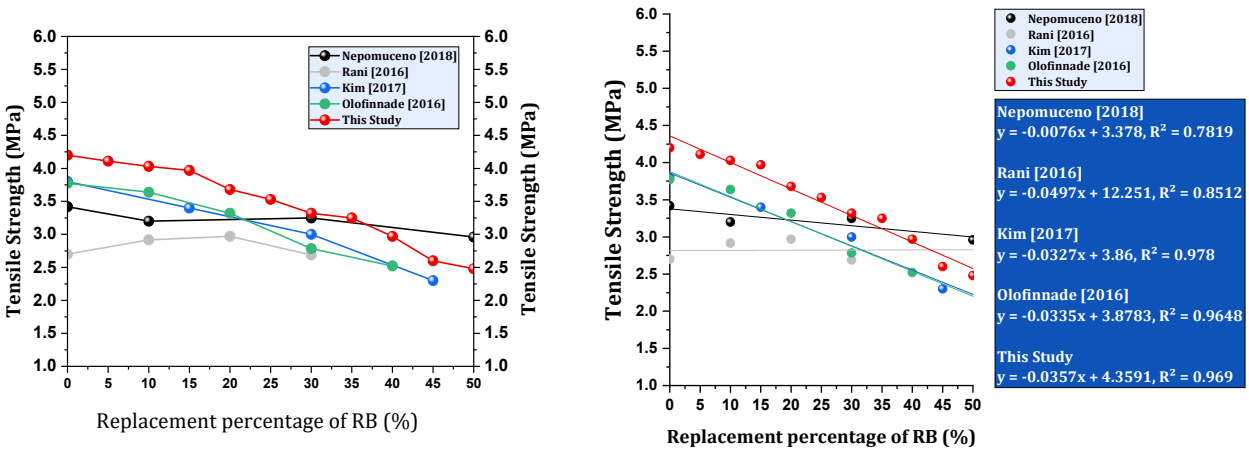

(**a**) (**b**)

Figure 17. Prior research on tensile strength [49,50,101,102]: (**a**) Impact of brick powder; (**b**) Regression analysis of tensile strength versus varying brick powder doses.

4.1.5. Impact Strength—First Crack Strength & Failure Strength

The average results for the first crack strength and failure strength are illustrated in Figure 18. This figure provides a comparative analysis of how different percentages of brick powder affect these key properties. Additionally, Figure 19 details the impact strength of the mixtures with varying brick powder ratios in comparison to the control mixture. This information highlights how the inclusion of brick powder influences the overall impact resistance of the concrete.

The average strength of the first crack for the control mixture was measured at 56 blows (Figure 18a). In contrast, the average range of the first crack strength for mixtures containing brick powder fell within the range of 31 to 54 blows. According to Figure 19, the replacement of brick powder instead of cement up to 15% resulted in a decrease in the resistance of the first crack by less than 10%. When 20% to 30% brick powder was used in the mixtures, a sharper drop in the strength of the first crack occurred, ranging from 14.29% to 28.57%. Substituting more than 30% of brick powder caused the first crack strength drop to exceed 30%, and at 50% replacement, the strength drop reached 44.65%.

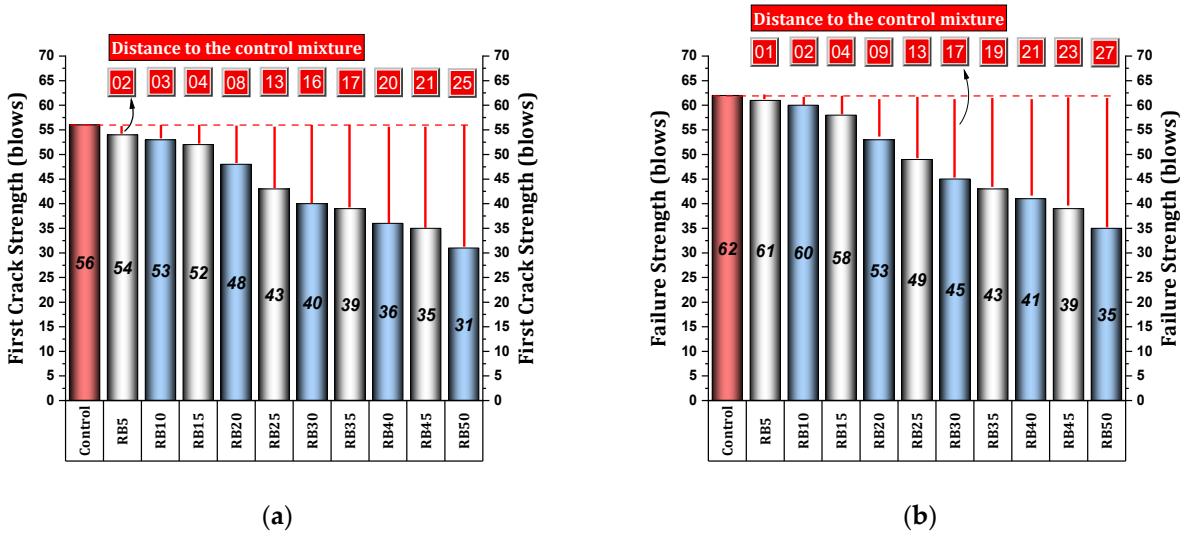

Figure 18. Average of impact strength: (**a**) First crack strength; (**b**) Failure strength.

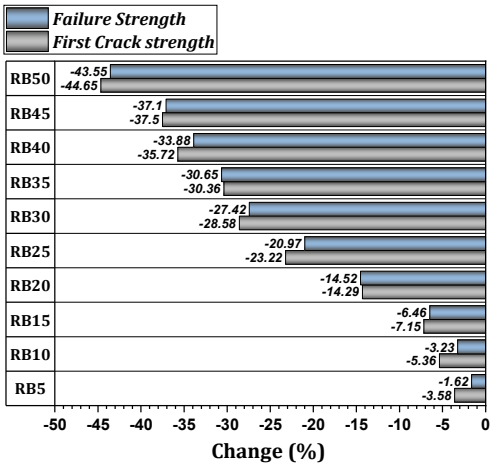

Figure 19. Percentage changes in impact strength.

According to Figure 18b, the average failure strength for the control mixture is 62 blows. The failure strength of mixtures containing brick powder followed a decreasing trend, similar to the strength of the first crack strength. Specifically, mixtures containing 5%, 10%, and 15% brick powder exhibit average failure strengths of 61, 60, and 58 blows, respectively, indicating a reduction range of 1% to 6% for this group of mixtures. When crossing the 20% replacement threshold for brick powder, there was a 14.52% decrease in the failure strength. Furthermore, at 30% replacement, the decrease in the failure strength exceeded 25%. Notably, the amount of reduction in the failure strength within the replacement range of 40% to 50% is evident, ranging from 33.88% to 43.55%.

4.1.6. Impact Strength—INPB, Impact Energy, and Ductility Index

The average INPB results for mixtures with varying percentages of brick powder are shown in Figure 20. For the control mixture, the INPB value was measured at 6 blows. This figure illustrates how different amounts of brick powder influence the impact resistance of the concrete mixtures. Substituting brick powder by 5% to 10% led to an increase in INPB to 7 blows, indicating an improvement of INPB by 16.67%. However, the replacement of 20% to 30% brick powder did not exhibit significant differences compared to the control mixture. Beyond a 35% replacement percentage, the INPB drop rate exceeded 30%. Notably, for mixtures with more than 40% replacement (specifically, the RB45 and RB50 mixtures), the INPB value decreased by 37% to 44%.

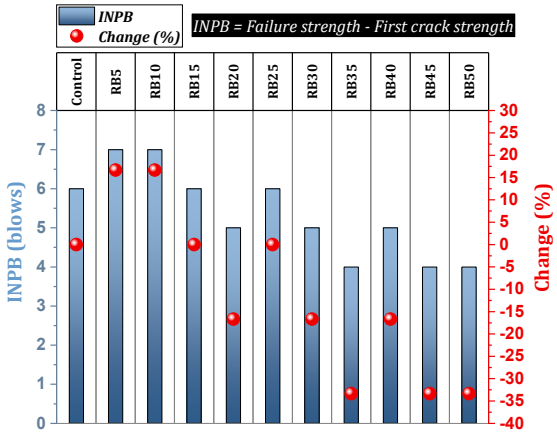

Figure 20. The INPB results.

The ability to absorb energy and the ductility index are depicted in Figure 21. For the control mixture, the impact energy value was 1140 J for the first crack strength and 1262 J for the failure strength, representing the best performance among all the mixtures. However, the ability to absorb energy exhibits a decreasing trend when brick powder replaces cement. While the impact energy reduction at low dosages of brick powder is typically insignificant, using high dosages results in a sharp reduction in energy absorption potential. Specifically, when 5% to 15% brick powder is used, there is a 7% reduction in energy absorption. As the replacement percentage of brick powder increases from 20% to 30%, the energy absorption decrease ranges from 14% to 28%. Beyond 40% replacement, the energy absorption decreases by more than 30%. Finally, the weakest performance, with an approximately 44% drop in energy absorption, is observed for the RB50 mixture. According to Figure 21, the ductility index has improved due to the replacement of brick powder. This finding suggests that brick powder possesses a positive effect on increasing the toughness of concrete mixtures (albeit this is less significant than the reduction in strength). The observed improvement may be attributed to the presence of brick particles, which provide a suitable substrate for cement mixture entanglement.

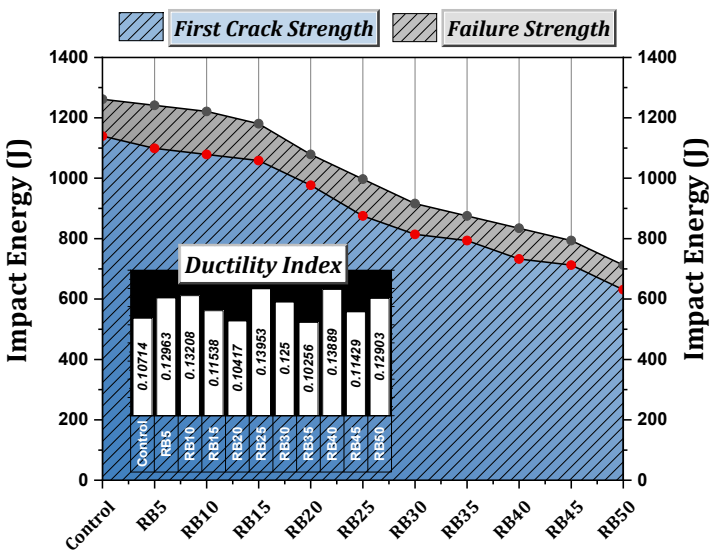

Figure 21. Impact energy and Impact ductility index results.

To the best of our knowledge, this study represents the first investigation of the impact strength properties of concrete containing recycled brick powder as a partial cement replacement. While several studies have examined the compressive, tensile, and flexural behavior of this type of concrete, the impact performance has not been previously reported

in the literature. Consequently, a review of studies on the impact of supplementary cementitious materials on effect resistance was undertaken. The study by Saradar et al. [11] demonstrated an enhancement in the INPB for mixtures containing single-component silica fume and a binary mixture of silica fume and nano-titanium. In this regard, the number of INPB blows for the single-component and binary mixtures was determined to be 6 and 7, respectively. Mohtasham Moein's study [52] revealed that employing recycled concrete powder (RCP) at dosages of 5% and 10% resulted in a 25% enhancement in the INPB. At dosages of 15% and 20% RCP, the INPB values were similar to the control mixture. However, for dosages exceeding 20% RCP, the INPB values decreased. An analysis of the impact energy data from this study indicates a declining trend in impact energy with increasing RCP dosages. Beshkari et al. [109] examined the influence of nano-silica (at dosages of 0.5% and 1%) and zeolite (at dosages of 5% and 10%) on the impact resistance of self-compacting concrete. The findings revealed that the INPB for the control mixture was 1 blow, whereas mixtures incorporating 0.5% and 1% nano-silica exhibited 2 and 3 blows, respectively. For mixtures containing zeolite, the INPB was recorded as 2 blows. The impact energy parameter demonstrated a 25% and 50% increase for mixtures containing 0.5% and 1% nano-silica, respectively. Moreover, mixtures containing 5% and 10% zeolite showed improvements of 12.5% and 33.34% in impact energy, respectively. Additionally, the ductility index for mixtures containing 0.5% and 1% nano-silica improved significantly by 66.112% and 111.416%, respectively. Similarly, the ductility index for mixtures containing 5% and 10% zeolite exhibited increases of 86.046% and 55.038%, respectively. The reduction in impact energy and INPB of concrete when using RBP is attributed to the distinct physical and chemical properties of this material compared to cement. RBP often exhibits higher porosity and lower mechanical strength than cement, leading to a decrease in the concrete's resistance to impact and dynamic loads. Conversely, zeolite and nano-silica, owing to their nanometer-scale structure and high specific surface area, can enhance the mechanical properties of concrete. These materials function as fine fillers within the concrete matrix, reducing porosity and accelerating pozzolanic reactions, which in turn increase the compressive, tensile, and flexural strengths of concrete. Consequently, the incorporation of zeolite and nano-silica can contribute to improved impact energy and INPB of concrete. Ismail et al. [110] also reported an improvement in the impact energy of self-compacting concrete containing binary combinations of fly ash, slag, silica fume, and metakaolin. Gupta et al. [111] investigated the impact resistance of reinforced concrete incorporating various percentages of waste rubber fibers and three different silica fume content groups: 0%, 5%, and 10%. The results indicated that increasing the dosage of silica fume could enhance the INPB, impact energy, and ductility.

4.2. Numerical Analysis

4.2.1. Prediction of Compressive Strength (By ANN and FL)

The average compressive strength at 28 days for all mixtures was analyzed using ANN and FL models. The results of the 28-day compressive strength, obtained from the testing process and predicted by the ANN and FL algorithms, are reported in Figure 22. Examining the results solely based on the evaluation of Figure 22 indicates that the ANN model provides predictions closer to reality. However, this alone cannot serve as conclusive evidence of the ANN model's superior performance compared to FL. To further assess the model's accuracy, the prediction errors relative to the actual results were examined. Figure 23 illustrates the prediction error of the ANN model in comparison to the actual results, with an average prediction error of 0.87%. In contrast, Figure 23 displays the prediction error of the FL model, which has an average error of 4.66%. The results reveal that the ANN model's prediction error rate is 3.79% lower than that of FL. Consequently, while the ANN model offers more accurate predictions, the performance of the FL model in predicting compressive strength should not be disregarded. Figure 24 illustrates the relationship between the experimentally measured strength and the strength predicted by ANN and FL models. The findings reveal a more robust correlation between the ANN model results and

the laboratory measurements compared to the FL model. The performance of the ANN model for training, validation, testing, and all datasets is depicted in Figure 25. Based on the regression coefficient extracted from the ANN model (greater than 0.98), the model can be said to possess a high ability to predict experimental results. Table 9 presents a report of the statistical measures obtained for the ANN model. The evaluation metrics for the predictive model of compressive strength demonstrate its exceptional performance. The R of 0.99123 suggests an almost perfect positive linear relationship between the predicted and actual compressive strengths, indicating that the model's predictions are closely aligned with the observed data. The MSE of 0.15628 MPa^2 provides an average of the squared differences between actual and predicted values, though it is less intuitive than the RMSE, which stands at 0.39533 MPa. This RMSE highlights that the average prediction error is about 0.398 MPa, reflecting great accuracy, as the typical prediction is very close to the true value. The MAE of 0.39137 MPa corroborates this finding, as it indicates a similar average prediction error without the influence of squaring differences, suggesting consistent errors without significant outliers. Furthermore, the SI of 0.86%, signifies outstanding precision in the model, as it indicates a minimal spread of predictions around the actual values. Finally, the OBJ value of 0.398 MPa, derived from RMSE, reinforces the model's strong predictive ability, with lower values signaling enhanced performance. Overall, these metrics collectively affirm the model's reliability in predicting compressive strength.

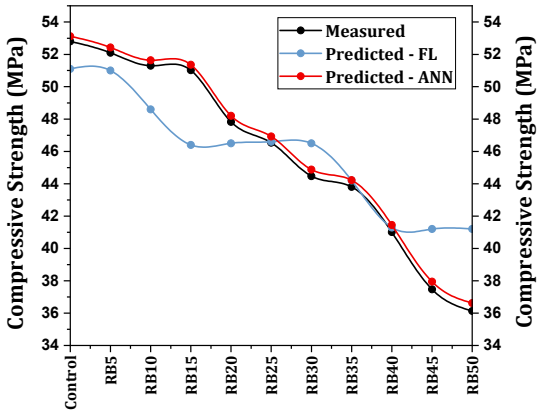

Figure 22. The comparisons of the measured and predicted compressive strengths with FL and ANN.

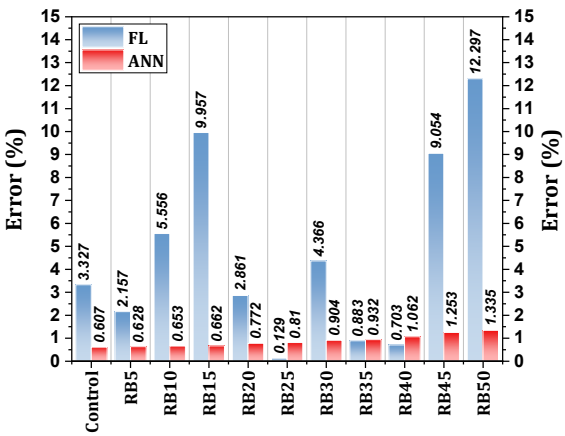

Figure 23. Prediction error by ANN and FL model compared to reality.

Table 9. Summary of statistical measures for the model evaluation.

R	MSE	RMSE	MAE	SI	OBJ
0.99	0.15	0.39	0.39	0.86	0.39

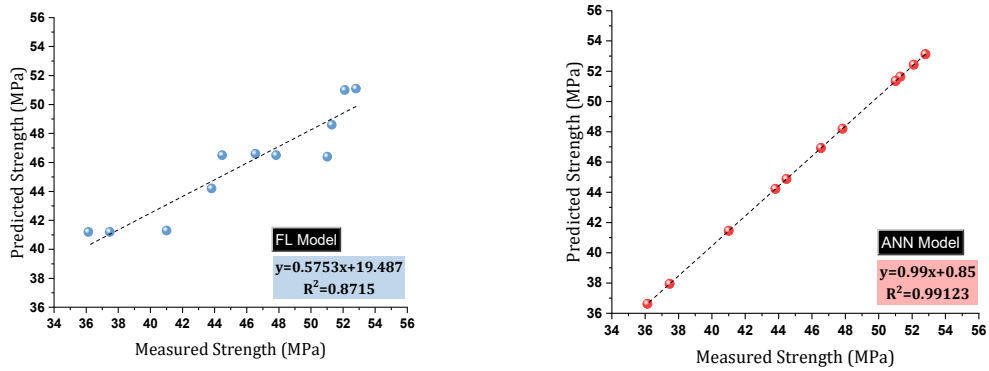

(**a**) (**b**)

Figure 24. The correlation of the measured and predicted compressive strengths: (**a**) FL model; (**b**) ANN model.

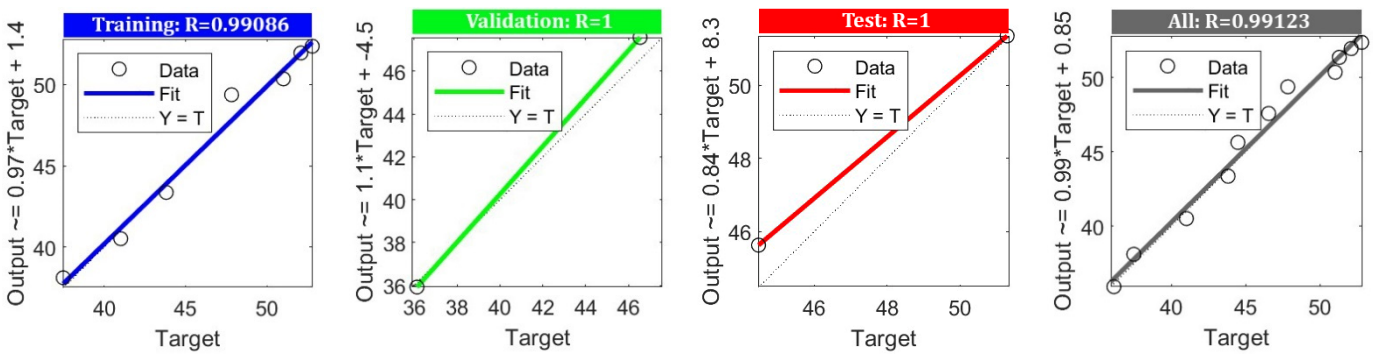

(**a**) (**b**) (**c**) (**d**)

Figure 25. The performance of the ANN model: (**a**) the training; (**b**) the validation; (**c**) the test; (**d**) all datasets.

4.2.2. Statistical Analysis of Impact Data (By Weibull Distribution)

Researchers [34,42,43] have considered employing statistical methods to interpret the results of the RDWI test in order to address the challenge of significant data dispersion previously mentioned. Table 10 provides an overview of various statistical methods for analyzing impact test results. Damage resulting from impact forces can be treated as a random distribution variable that must adhere to specific statistical principles. The Weibull distribution model is defined as shown in Equation (5):

$$f(x) = \frac{\beta}{\eta}\left[\frac{x - x_0}{\eta}\right]^{\beta-1} \exp\left\{-\left[\frac{x - x_0}{\eta}\right]^{\beta}\right\}(x \geq x_0) \tag{5}$$

In Equation (5): β—Shape factor; η—Scale factor; X_0—Location parameters ($X_0 \geq 0$). The similarity between the failure mechanisms caused by impact and fatigue forms the foundation for modeling impact life, denoted as (N), using the Weibull distribution. However, the three primary parameters require redefinition. Specifically, we set β = b, η = $N_a - N_0$, and $X_0 = N_0$. Ultimately, the impact life (N) can be described by the probability density function given in Equation (6):

$$f(N) = \frac{\beta}{N_a - N_0}\left[\frac{N - N_0}{N_a - N_0}\right]^{b-1} \exp\left\{-\left[\frac{N - N_0}{N_a - N_0}\right]^{b}\right\}(\infty > N \geq N_0) \tag{6}$$

Table 10. Statistical methods employed by researchers in RDWI testing of various concrete types.

No.	Concrete Type	Discs	Statistical Technique	Ref.
1	Steel fiber-reinforced concrete	15	-Normal Probability	[112]
2	Fiber-reinforced concrete	32	-Normal Probability -Kolmogorov–Smirnov test -Kruskal–Wallis test	[43]
3	High strength fiber-reinforced concrete	32	-Normal Probability -Kolmogorov–Smirnov test -Kruskal–Wallis test	[32]
4	High strength fiber-reinforced concrete	48	-Normal Probability -Kolmogorov–Smirnov test	[113]
5	Hybrid fiber-reinforced concrete	48	-Normal Probability -Kolmogorov–Smirnov test	[42]
6	Steel fiber-reinforced concrete	6	-Two-parameter Weibull distribution	[114]
7	Multi-layered prepacked aggregate fibrous composite	6		[115]
8	Multiphase lightweight aggregate concrete	6		[116]
9	High-performance cement composites with pozzolan	8		[11]
10	Self-compacting concrete containing waste tiles	12		[109]
11	Two-stage fiber-reinforced concrete	15		[82]
12	Polyolefin fiber-reinforced concrete	32		[34]

In Equation (6): b—Weibull shape parameters; N_0—Minimum life parameter; N_a—Characteristic life parameters. In this context, the cumulative distribution function $F(N_p)$ is defined as follows according to Equation (7):

$$F(N_p) = P_1(N < N_p) = \int_{N_0}^{N_P} f(N)dN = 1 - \exp\left\{-\left[\frac{N_p - N_0}{N_a - N_0}\right]^b\right\} \tag{7}$$

The parameter P_1 ($N < N_p$) in Equation (7) represents the probability that N_p is less than a certain value. The function associated with $F(N_p)$ is referred to as the cumulative probability of failure. Additionally, the reliability function P_2 is defined by Equation (8):

$$P_2 = P_1(N > N_p) = 1 - F(N_P) = \exp\left\{-\left[\frac{N_p - N_0}{N_a - N_0}\right]^b\right\} \tag{8}$$

By utilizing Equation (8), the impact life N_P can be computed given the occurrence of a P_1 failure. Taking into account the reliability of the sample during the service process and simplifying the equation, we set the parameter N_0 equal to 0. In this scenario, the two-parameter Weibull probability density function is derived. The corresponding function is expressed as follows according to Equation (9):

$$f(N) = \frac{b}{N_a}\left[\frac{N}{N_a}\right]^{b-1} \exp\left\{-\left[\frac{N}{N_a}\right]^b\right\} (\infty \geq N > N_0) \tag{9}$$

Next, the failure probability function (P_1) for the case when $N > N_p$ is expressed as Equation (10):

$$P_1 = 1 - exp\left\{-\left[\frac{N}{N_a}\right]^b\right\} \tag{10}$$

Furthermore, the survival function (also known as the reliability function) denoted as (P_2) can be determined using Equation (11):

$$P_2 = 1 - P_1 = exp\left\{-\left[\frac{N}{N_a}\right]^b\right\} \tag{11}$$

By applying the natural logarithm to both sides of Equation (11), we can obtain Equation (12) as the output:

$$ln\left[ln\left(\frac{1}{P_2}\right)\right] = bln\left(\frac{1}{N_a}\right) + bln(N) \tag{12}$$

According to y = ln [ln(1/P_2)], x = ln (N), a = b ln N_a and N_a = exp [−(a/b)]; Equation (13) can be defined:

$$Y = a + bX \tag{13}$$

Equation (13) can be employed to verify whether the data's potential adheres to the distribution law of the Weibull probability density function. The parameters a and b appearing in Equation (13) are obtained through linear regression analysis. At this juncture, two scenarios for the linear relationship between X and Y can be envisioned: (i) the presence of a strong relationship, indicating that the Weibull probability density function reasonably predicts the lifespan of mixtures containing brick powder across various failure probabilities; (ii) the existence of a weak relationship, in which case the Weibull probability density function is ineffective for investigating and describing the impact life of such mixtures. A robust correlation between ln[ln(1/P_2)] and ln(N) is essential to provide a compelling justification for investigating the impact life of Weibull specimens. Consequently, the survival rate (P_2) must be computed, as defined by Equation (14):

$$P_2 = 1 - \frac{i}{t+1} \tag{14}$$

In Equation (14): i—represents the number of concrete discs and t—represents the total number of concrete discs used. Table 11, Figures 26 and 27 are derived from Equations (11)–(14), with X representing the abscissa, Y denoting the ordinate, and the regression parameters are also taken into account.

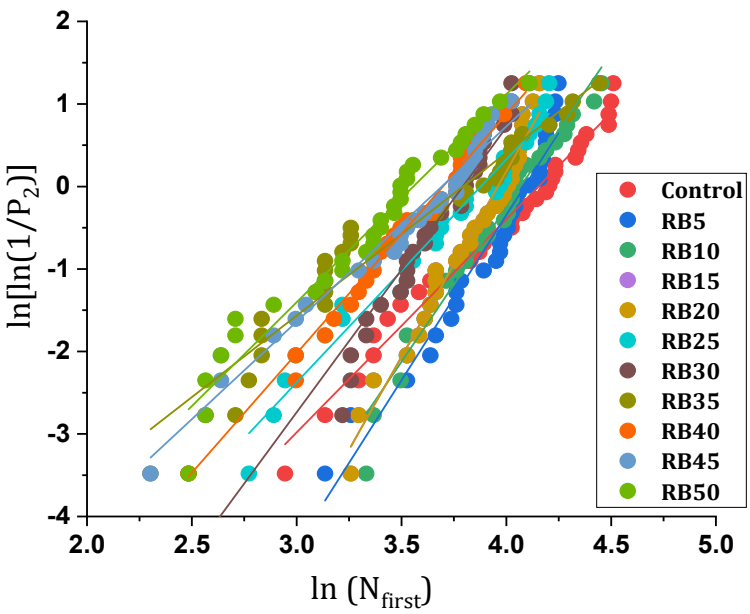

Figure 26. Weibull lines for first crack strength.

Table 11. Weibull parameters computed for mixtures.

First Crack Strength					
R^2	Intercept	Scale parameter, η	Shape parameter, β	Mix Code	N.O.
0.9805	−10.734	63.6693	2.5842	Control	1
0.9542	−16.36	59.557	4.003	RB5	2
0.971	−15.219	58.4114	3.7416	RB10	3
0.9357	−17.23	57.497	4.2525	RB15	4
0.9724	−17.802	52.4321	4.496	RB20	5
0.9722	−10.489	48.3444	2.7045	RB25	6
0.9332	−13.098	44.3749	3.4535	RB30	7
0.946	−7.49	44.397	1.9746	RB35	8
0.98	−10.714	40.3686	2.8972	RB40	9
0.9745	−8.7304	40.1488	2.3643	RB45	10
0.9591	−8.9609	35.0543	2.5193	RB50	11
Failure strength					
R^2	Intercept	Scale parameter, η	Shape parameter, β	Mix Code	N.O.
0.9804	−12.667	69.6844	2.9847	Control	1
0.9736	−20.655	66.3378	4.924	RB5	2
0.9612	−17.279	65.773	4.1276	RB10	3
0.9637	−21.459	62.6451	5.1881	RB15	4
0.9731	−20.296	58.1658	4.9949	RB20	5
0.9718	−13.047	54.4878	3.2634	RB25	6
0.9329	−14.678	49.8296	3.7553	RB30	7
0.9275	−8.7004	49.0649	2.2348	RB35	8
0.9822	−14.945	45.3339	3.9184	RB40	9
0.9532	−10.102	44.448	2.6624	RB45	10
0.9525	−10.441	39.179	2.8464	RB50	11

Upon analyzing the results from Table 11, it is evident that the highest regression coefficient R^2 was achieved for the RB40 mixture (with R^2 = 0.98). Taking a broader perspective, it can be inferred that the R^2 values for all mixtures exceed 0.9081. Statistically speaking, an acceptable model should exhibit an R^2 greater than 0.7 [34,43]. Based on the findings from mixtures containing brick powder, the linear regression fit is established. Consequently, the impact test results align with the distribution law of the Weibull probability density function, affirming the validity and reliability of the equation (Y = a + bX). Equation (15) can be derived through the deformation of Equations (12)–(14). This equation provides an estimate for the impact life of mixtures containing varying proportions of brick powder across different failure probabilities, denoted as P_1:

$$N = exp\left\{\frac{\ln[\ln(1/(1-P_1))] - a}{b}\right\} \tag{15}$$

From Table 11, the parameters a and b are extracted. Additionally, using Equation (15), the impact of life at various failure probabilities (P_1) is determined. Finally, the estimated impact life for mixtures containing different proportions of brick powder across varying failure probabilities (P_1) is obtained. These results are presented in Figure 28.

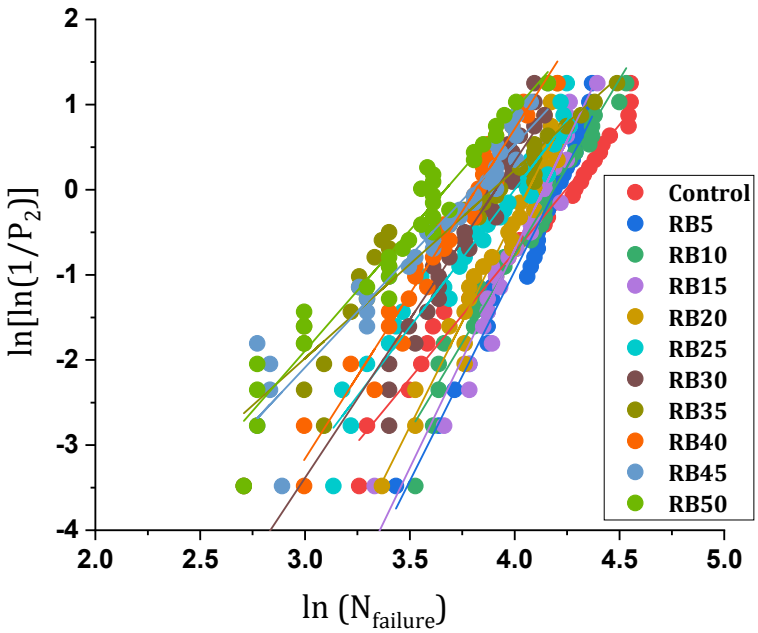

Figure 27. Weibull lines for failure strength.

4.2.3. Impact–Damage Analysis

Analyzing the impact life of mixtures containing varying proportions of brick powder across different failure probabilities using the Weibull probability density function does not yield a comprehensive view of the damage progression (from initial impact to final damage) in these mixtures. Consequently, to gain a clearer understanding of the path experienced by the concrete disc, the macroscopic damage evolution law was investigated by incorporating an impact–damage model based on the Weibull distribution for these mixtures. Upon analyzing the resulting curves, it becomes evident that the function value of the Weibull distribution's failure probability function gradually increases. This behavior is influenced by the rise in drop-hammer-impact occurrences. The trajectory followed by the concrete disc during damage-induced impact reveals the correlation between impact damage severity and the count of applied blows. Notably, each impact on the concrete disc contributes to its weakening, thereby enhancing the influence of subsequent blows. The cumulative effect of increasing the number of blows leads to fatigue in the concrete disc.

Concrete exhibits both strength and fragility. While it can endure sustained forces, sudden impacts may result in cracks and vulnerabilities. Initially imperceptible, these cracks signify cumulative damage from repeated impacts. Each traumatic event adds another layer of weakness atop the effects caused by prior incidents. This repeated stress leads to a phenomenon known as fatigue. Analogous to how metal deforms and fractures due to repeated bending, concrete also weakens over time and eventually reaches the failure stage due to recurrent impacts. Consequently, with each impact, the likelihood of concrete failure increases. As damage accumulates, the concrete grows progressively weaker, ultimately diminishing its ability to withstand force before breaking.

The failure probability of concrete, denoted as $P_F(n)$, and the damage degree, represented by $D(n)$, are defined after a series of n blows. When a concrete disc deteriorates due to repeated hammer impacts, both $P_F(n)$ and $D(n)$ assume a value of 1. Drawing upon the Weibull distribution, the impact–damage model is formulated for mixtures containing varying proportions of brick powder, as expressed in Equation (16):

$$D(n) = 1 - exp\left[-\left(\frac{n}{\eta}\right)^{\beta}\right] \tag{16}$$

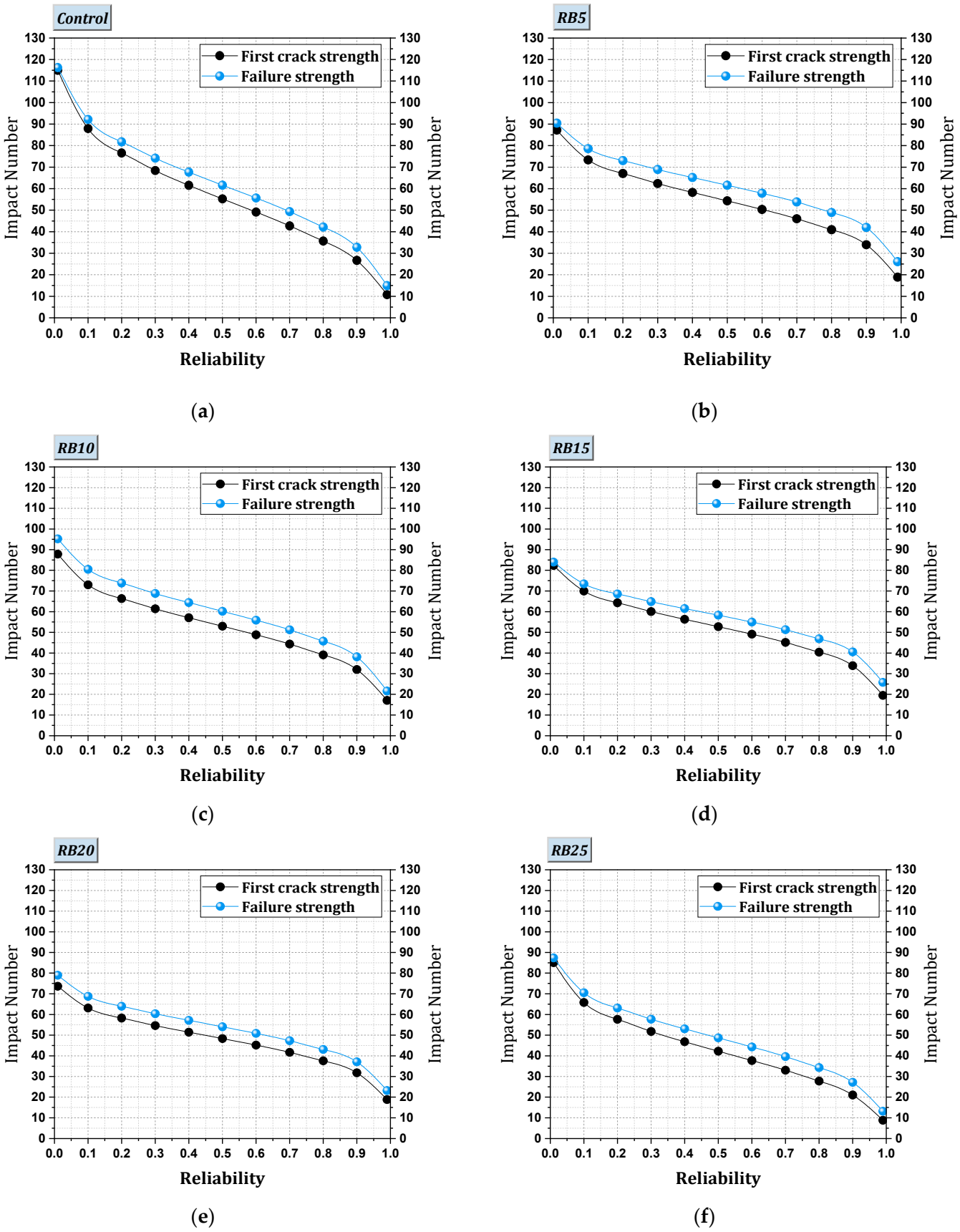

Figure 28. *Cont.*

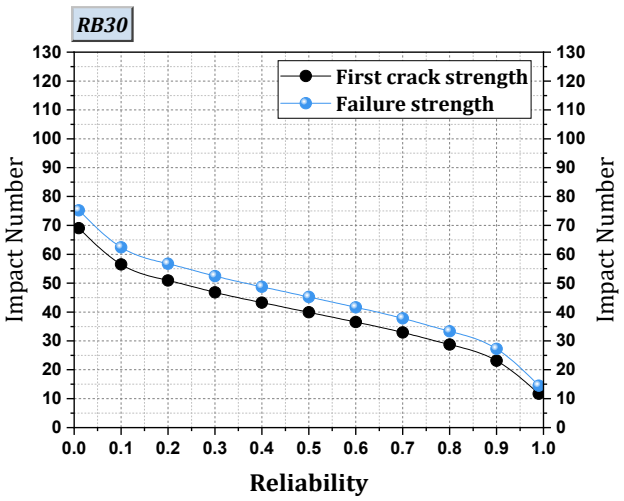

(g)

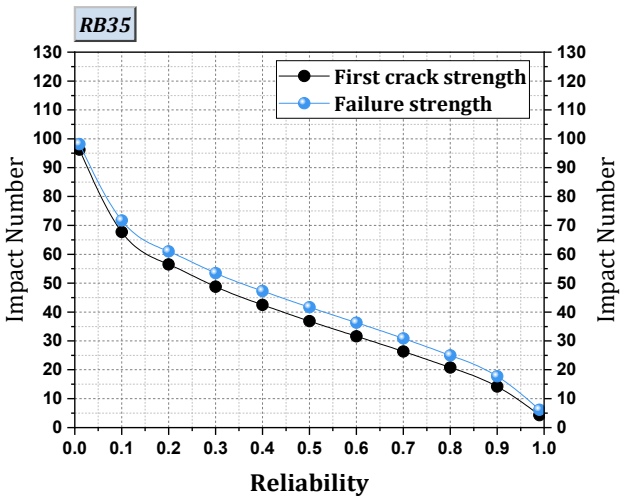

(h)

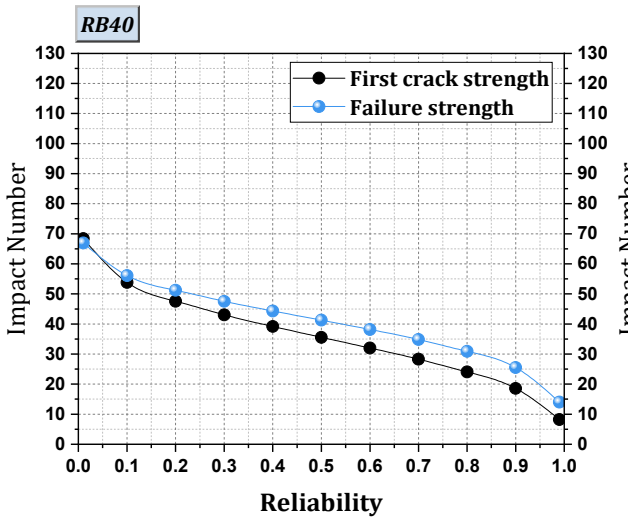

(i)

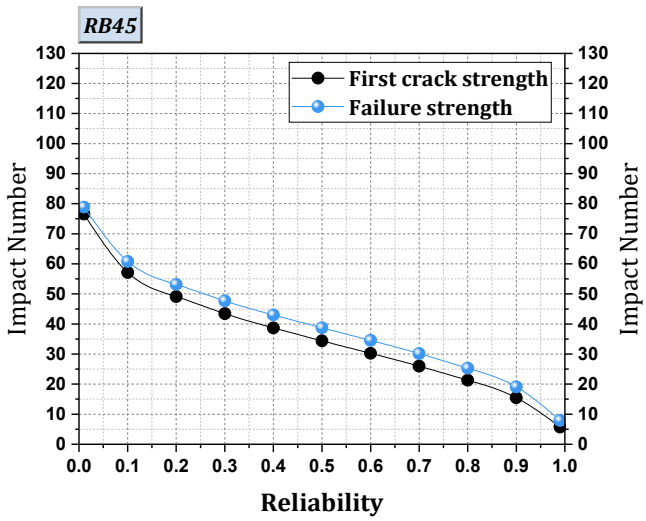

(j)

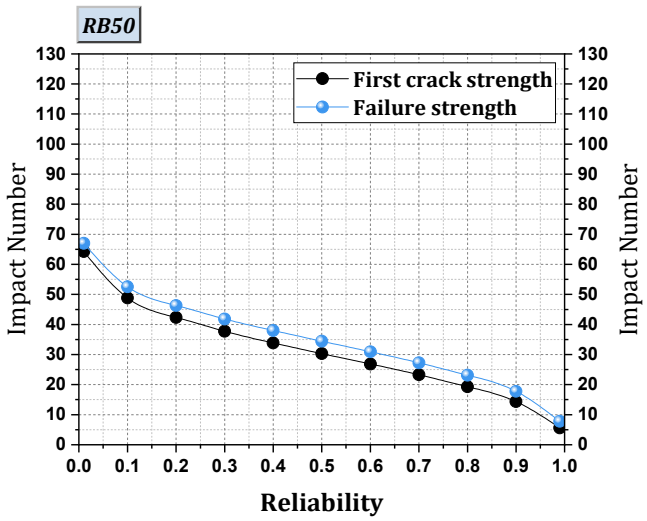

(k)

Figure 28. Impact strength corresponding to reliability level: (**a**) control; (**b**) RB5; (**c**) RB10; (**d**) RB15; (**e**) RB20; (**f**) RB25; (**g**) RB30; (**h**) RB35; (**i**) RB40; (**j**) RB45; (**k**) RB50.

In Equation (16), n represents the number of blows on the concrete disc, while β and η correspond to the shape and scale parameters previously discussed. Figure 29 illustrates distinct stages within the impact–damage–evolution diagram. The impact–damage–evolution diagram, which pertains to various concrete mixtures, is depicted in Figure 30. Based on the curves within this diagram, three discernible stages emerge. In the initial stage, the impact damage remains minimal, primarily influenced by pore expansion and micro-crack propagation. During stage 2, the joining of micro-cracks results in wider fissures and more severe damage. If concrete mixtures incorporate fibers, these materials exhibit a bridging property, leading to an expanded stage 2 in the curve. Ultimately, as cracks accumulate and the concrete disc surpasses its fatigue capacity, stage 3 commences, culminating in concrete failure. When the damage degree attains a value of 1 (D(n) = 1), the concrete disc fractures completely, reaching the fracture stage.

According to Figure 30a, there is a negligible difference in the behavior of the RB5 and RB10 mixtures compared to the control mixture. Based on Figure 30b, as the substitution of RBP increases within the range of 15–20% (RB15 and RB20), the behavioral differences of the graphs gradually become apparent under the influence of RBP. In this context, the behavior of the concrete disc faces challenges against repeated impacts, and due to the presence of RBP in its structure, it exhibits lower fatigue capacity compared to the control mixture. As evident from Figure 30c,d, the control mixture exhibits a wider profile from the second stage compared to the mixtures containing RBP, demonstrating greater fatigue capacity against impacts. When the substitution percentage of RBP was selected within the range of 45–50%, as shown in Figure 30e, the graphs diverged more distinctly from the control mixture, indicating an increased tendency to transition more rapidly through the three stages.

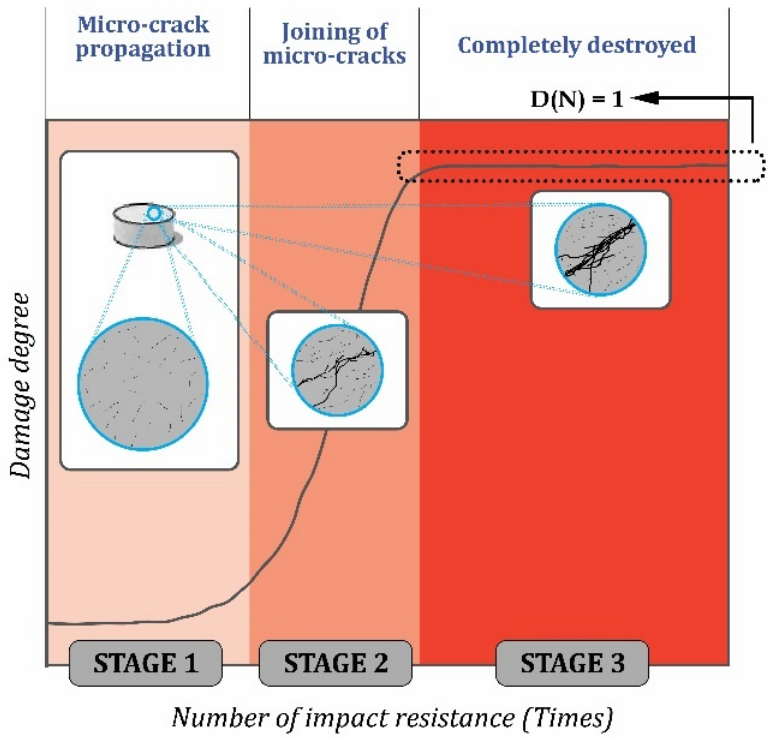

Figure 29. Different stages of an impact–damage–evolution diagram.

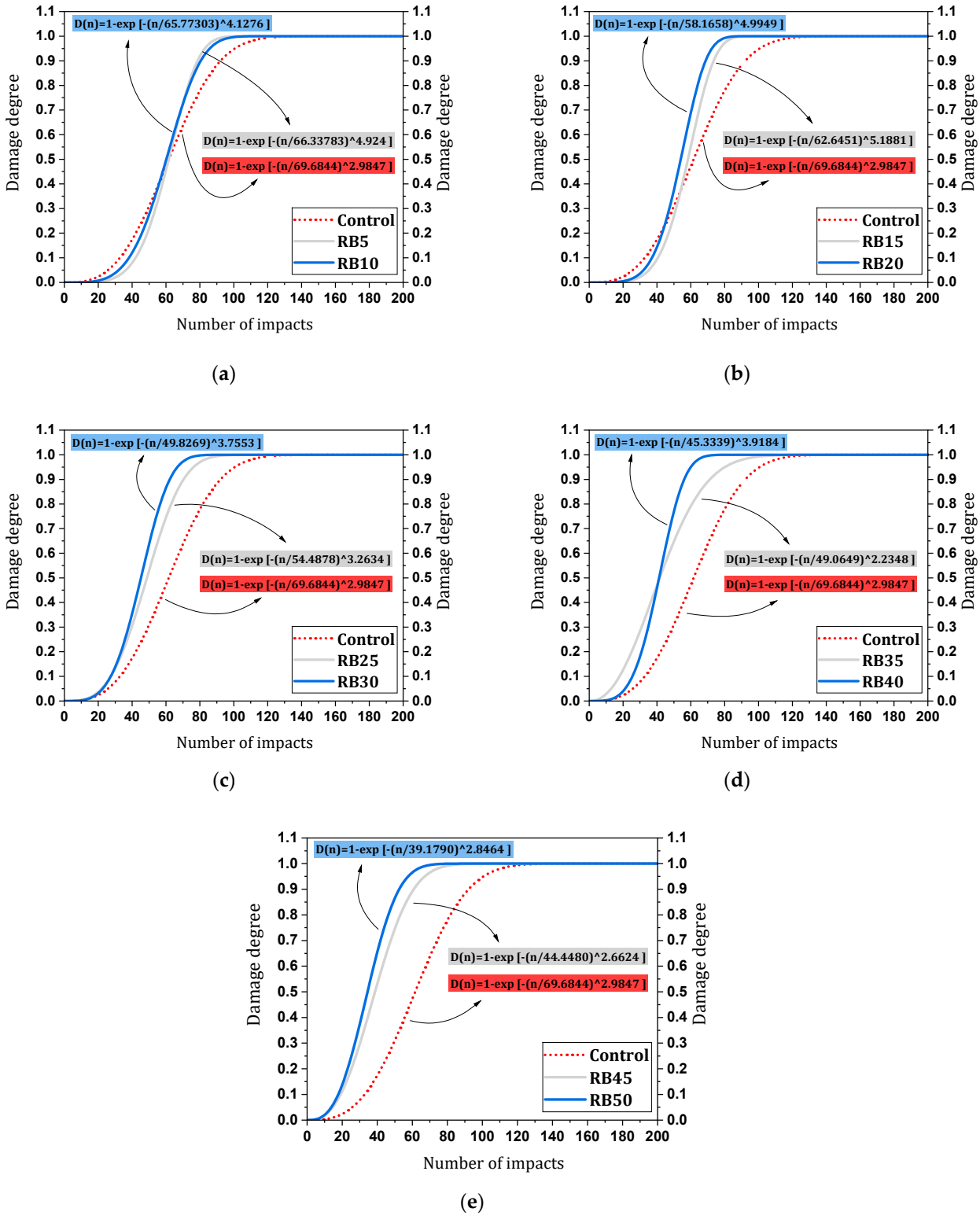

Figure 30. Impact–damage–evolution diagram for mixtures containing brick powder compared to the control mixture: (**a**) RB5 & RB10; (**b**) RB15 & RB20; (**c**) RB25 & RB30; (**d**) RB35 & RB40; (**e**) RB45 & RB50.

5. Conclusions

This study investigates the effect of various percentages (5–50%) of brick powder on compressive, flexural, tensile, and impact strength. In this process, methods such as ANN, FL, and Weibull analysis were employed. The results were obtained as follows:

- Compressive strength is negatively affected by brick powder substitution. Mixtures with up to 15% brick powder maintain strength, with a slight decline of 1.33% to 3.38%. Beyond this threshold, the decrease in compressive strength becomes significant, exceeding 30% for 50% brick powder replacement.
- Flexural strength remains acceptable with up to 15% brick powder replacement, experiencing a maximum reduction of 3.94%. However, substituting 25% of cement with brick powder results in a reduction exceeding 10%. Higher proportions lead to a significant decline, reaching 22.45% at a 50% replacement rate.
- Tensile strength decreases with brick powder substitution. Replacing 5%, 10%, and 15% of cement with brick powder results in reductions of 2.15%, 4.05%, and 5.48%, respectively. A decrease of over 10% occurs at a 20% replacement level, with reductions of 30–41% noted at 40–50% substitution.
- Impact strength shows a noticeable decline with increased brick powder content. Substituting up to 15% of cement results in a reduction of slightly less than 10% in the first crack strength. Higher ratios (20% to 30%) lead to reductions of 14.29% to 28.57%, with a significant decrease of 44.65% for 50% replacement. Mixtures containing 5%, 10%, and 15% brick powder exhibit a slight decrease (1% to 6%) in the failure strength while mixtures exceeding 20% result in a reduction of 14.52%. Notably, the reduction increases significantly within the 40% to 50% range, reaching 33.88% to 43.55%.
- Substituting 5% to 10% of cement with brick powder improves INPB by nearly 17%. Replacements of 5% to 15% slightly decrease energy absorption by about 7%. Higher substitution rates significantly reduce energy absorption by 30% to 44%, while brick powder notably increases the mixture's ductility index.
- The ANN model accurately forecasts compressive strength, achieving an average error of only 0.87%. In contrast, the FL model has a larger average error of 4.66%. The strong relationship between the predictions made by the ANN model and the actual results is reflected in its regression coefficient, which exceeds 0.98, demonstrating the model's effectiveness in predicting experimental results.
- RDWI test outcomes for brick powder mixtures align with the two-parameter Weibull distribution. An equation based on this model accurately predicts impact damage evolution, correlating well with experimental data and confirming the model's dependability in detailing damage progression under repeated impacts.

6. Limitations and Guide for Future Studies

The integration of machine learning techniques, particularly ANN and FL, has shown promise in identifying compressive strength behavior in concrete. However, further exploration of alternative models could enhance design processes. ANNs excel at handling nonlinear relationships through empirical data learning, while FL relies on expert knowledge for rule-based information. Key advantages of ANNs include the absence of a predefined mathematical model, support for both supervised and unsupervised learning, and the ability to learn from experiential data, though they do not extract explicit rules. Conversely, FL does not require a mathematical model but relies on expert-defined rules, lacking formal learning algorithms. The combination of ANNs and FL, particularly in neuro-fuzzy systems, is recommended for effectively modeling complex systems with limited prior information. Future research should explore cooperative, concurrent, and hybrid neuro-fuzzy systems, each offering unique collaborative approaches to enhance learning capabilities. There is also a need to investigate the Sugeno approach in FL for concrete technology, as most studies have focused on the Mamdani approach. Additionally, future studies should examine the long-term durability of concrete containing RBP and the application of various types of fibers and new materials, such as graphene oxide, in RBP-reinforced concrete, which has yet to be explored.

Author Contributions: The contribution is the result of the joint work of the authors. In particular: Conceptualization, M.M.M. and A.S.; methodology, M.M.M., K.R., A.M.M., A.S., S.E.R. and A.A.T.; software, M.M.M., K.R., A.M.M., A.S., S.E.R. and A.A.T.; validation, M.M.M., K.R., A.M.M. and A.S.; formal analysis, M.M.M., A.M.M. and A.S.; investigation, M.M.M. and A.S.; resources, M.M.M. and A.S.; data curation, M.M.M. and A.S.; writing—original draft preparation, M.M.M., K.R., A.M.M. and A.S.; writing—review and editing, M.M.M., A.S., S.E.R. and A.A.T.; visualization, M.M.M., K.R. and A.M.M.; supervision, M.M.M. and A.S.; project administration, M.M.M. and A.S. All authors have read and agreed to the published version of the manuscript.

Funding: This research received no external funding.

Data Availability Statement: The dataset analyzed during the current study is available and can be provided upon request.

Conflicts of Interest: Author Sam E. Rigby was employed by the company Arup Resilience, Security & Risk. The remaining authors declare that the research was conducted in the absence of any commercial or financial relationships that could be construed as a potential conflict of interest.

Abbreviations

ACI	American Concrete Institute
ASTM	American Society for Testing and Materials
ANN	Artificial neural network
C&D	Construction and demolition
CO_2	Carbon dioxide
CH_4	Methane
$D(n)$	Damage degree
d_{ij}	Desired output of the network for sample i in processed element j
E	Energy absorption
FL	Fuzzy logic
F-gases	Fluorinated gases
$F(N_p)$	Cumulative distribution function
g	Gravitation acceleration
GHG	Global greenhouse gas
G20	Group of twenty
h	Height of drop
i	Number of concrete discs
IDI	Impact ductility index
INPB	Increase in the number of post-first crack blows
ITZ	Interfacial transition zone
MSE	Mean squared error
m	Mass of hammer
N	Impact life
N_2O	Nitrous oxide
N_0	Minimum life parameter
N_a	Characteristic life parameters
N_{first}	First visual crack
$N_{failure}$	ultimate crack
SD.	Standard deviation
P_2	Survival rate
P_1	Different failure probabilities
$P_F(n)$	Failure probability
RP	Recycled powder
RDWI	Repeated drop weight impact
RPC	Reactive powder concrete
RBP	Recycled brick powder
RCP	Recycled concrete powder
R^2	Coefficient of determination

t	Total number of concrete discs
X_0	Location parameters
y	Actual values
$\hat{y}$	Predicted values
$\tilde{y}$	Average values
y_{ij}	Network output for sample i in processed element j
β	Shape factor

References

1. Crippa, M.; Guizzardi, D.; Pagani, F.; Banja, M.; Muntean, M.; Schaaf, E.; Becker, W.; Monforti-Ferrario, F.; Quadrelli, R.; Risquez Martin, A.; et al. *GHG Emissions of All World Countries*; European Commission: Luxembourg, 2023.
2. Sun, X.; Li, Z.; Cheng, X.; Guan, C.H.; Han, M.; Zhang, B. Global Anthropogenic CH4 Emissions from 1970 to 2018: Gravity Movement and Decoupling Evolution. *Resour. Conserv. Recycl.* **2022**, *182*, 106335. [CrossRef]
3. Mohammad Nezhad Ayandeh, M.H.; Ghodousian, O.; Mohammad Nezhad, H.; Mohtasham Moein, M.; Saradar, A.; Karakouzian, M. Steel Slag and Zeolite as Sustainable Pozzolans for UHPC: An Experimental Study of Binary and Ternary Pozzolan Mixtures under Various Curing Conditions. *Innov. Infrastruct. Solut.* **2024**, *9*, 265. [CrossRef]
4. Oxford Economics. *Oxford Economics Future of Construction: A Global Forecast for Construction to 2030*; Oxford Economics: London, UK, 2021.
5. Statista. *Statista Construction Industry Spending Globally 2025*; Statista: Hamburg, Germany, 2019.
6. Tajasosi, S.; Saradar, A.; Barandoust, J.; Mohtasham Moein, M.; Zeinali, R.; Karakouzian, M. Multi-Criteria Risk Analysis of Ultra-High Performance Concrete Application in Structures. *CivilEng* **2023**, *4*, 1016–1035. [CrossRef]
7. Heyran Najafi, M.R.; Saradar, A.; Mohtasham Moein, M.; Karakouzian, M. Investigation Mechanical Characteristics and Permeability of Concrete with Pozzolanic Materials: A Sustainable Approach. In *Multiscale and Multidisciplinary Modeling, Experiments and Design*; Springer: Berlin/Heidelberg, Germany, 2024. [CrossRef]
8. Alyaseen, A.; Poddar, A.; Kumar, N.; Haydar, K.; Khan, A.; Sihag, P.; Lee, D.; Kumar, R.; Singh, T. Influence of Silica Fume and Bacillus Subtilis Combination on Concrete Made with Recycled Concrete Aggregate: Experimental Investigation, Economic Analysis, and Machine Learning Modeling. *Case Stud. Constr. Mater.* **2023**, *19*, e02638. [CrossRef]
9. Mohtasham Moein, M.; Rahmati, K.; Saradar, A.; Moon, J.; Karakouzian, M. A Critical Review Examining the Characteristics of Modified Concretes with Different Nanomaterials. *Materials* **2024**, *17*, 409. [CrossRef]
10. Tam, V.W.Y.; Soomro, M.; Evangelista, A.C.J. A Review of Recycled Aggregate in Concrete Applications (2000–2017). *Constr. Build. Mater.* **2018**, *172*, 272–292. [CrossRef]
11. Saradar, A.; Rezakhani, Y.; Rahmati, K.; Johari Majd, F.; Mohtasham Moein, M.; Karakouzian, M. Investigating the Properties and Microstructure of High-Performance Cement Composites with Nano-Silica, Silica Fume, and Ultra-Fine TiO2. *Innov. Infrastruct. Solut.* **2024**, *9*, 84. [CrossRef]
12. Mousavinejad, S.H.G.; Saradar, A.; Jabbari, M.; Moein, M.M. Evaluation of Fresh and Hardened Properties of Self-Compacting Concrete Containing Different Percentages of Waste Tiles. *J. Build. Pathol. Rehabil.* **2023**, *8*, 81. [CrossRef]
13. Nabighods, K.; Saradar, A.; Mohtasham Moein, M.; Mirgozar Langaroudi, M.A.; Byzyka, J.; Karakouzian, M. Evaluation of Self-Compacting Concrete Containing Pozzolan (Zeolite, Metakaolin & Silica Fume) and Polypropylene Fiber against Sulfate Attacks with Different PH: An Experimental Study. *Innov. Infrastruct. Solut.* **2023**, *9*, 1. [CrossRef]
14. Tavakoli, D.; Hashempour, M.; Heidari, A. Use of Waste Materials in Concrete: A Review. *Pertanika J. Sci. Technol.* **2018**, *26*, 499–522.
15. Tavakoli, D.; Sakenian Dehkordi, R.; Divandari, H.; de Brito, J. Properties of Roller-Compacted Concrete Pavement Containing Waste Aggregates and Nano SiO2. *Constr. Build. Mater.* **2020**, *249*, 118747. [CrossRef]
16. Mansoori, A.; Mohtasham Moein, M.; Mohseni, E. Effect of Micro Silica on Fiber-Reinforced Self-Compacting Composites Containing Ceramic Waste. *J. Compos. Mater.* **2020**, *1*, 95–107. [CrossRef]
17. Wu, H.; Zuo, J.; Zillante, G.; Wang, J.; Yuan, H. Construction and Demolition Waste Research: A Bibliometric Analysis. *Archit. Sci. Rev.* **2019**, *62*, 354–365. [CrossRef]
18. Yue, G.; Ma, Z.; Liu, M.; Liang, C.; Ba, G. Damage Behavior of the Multiple ITZs in Recycled Aggregate Concrete Subjected to Aggressive Ion Environment. *Constr. Build. Mater.* **2020**, *245*, 118419. [CrossRef]
19. He, Z.; Shen, A.; Wu, H.; Wang, W.; Wang, L.; Yao, C.; Wu, J. Research Progress on Recycled Clay Brick Waste as an Alternative to Cement for Sustainable Construction Materials. *Constr. Build. Mater.* **2021**, *274*, 122113. [CrossRef]
20. Tang, Q.; Ma, Z.; Wu, H.; Wang, W. The Utilization of Eco-Friendly Recycled Powder from Concrete and Brick Waste in New Concrete: A Critical Review. *Cem. Concr. Compos.* **2020**, *114*, 103807. [CrossRef]
21. Wong, C.L.; Mo, K.H.; Alengaram, U.J.; Yap, S.P. Mechanical Strength and Permeation Properties of High Calcium Fly Ash-Based Geopolymer Containing Recycled Brick Powder. *J. Build. Eng.* **2020**, *32*, 101655. [CrossRef]
22. Luo, X.; Gao, J.; Liu, X.; Li, S.; Zhao, Y. Hydration and Microstructure Evolution of Recycled Clay Brick Powder-Cement Composite Cementitious Materials. *J. Therm. Anal. Calorim.* **2022**, *147*, 10977–10989. [CrossRef]
23. Yang, D.; Liu, M.; Ma, Z. Properties of the Foam Concrete Containing Waste Brick Powder Derived from Construction and Demolition Waste. *J. Build. Eng.* **2020**, *32*, 101509. [CrossRef]

24. Sharmin, S.; Sarker, P.K.; Biswas, W.K.; Abousnina, R.M.; Javed, U. Characterization of Waste Clay Brick Powder and Its Effect on the Mechanical Properties and Microstructure of Geopolymer Mortar. *Constr. Build. Mater.* **2024**, *412*, 134848. [CrossRef]
25. Castillo, M.; Hernández, K.; Rodriguez, J.; Eyzaguirre, C. Low Permeability Concrete for Buildings Located in Marine Atmosphere Zone Using Clay Brick Powder. In Proceedings of the IOP Conference Series: Materials Science and Engineering, Chennai, India, 16–17 September 2020; Volume 758.
26. Wu, H.; Xiao, J.; Liang, C.; Ma, Z. Properties of Cementitious Materials with Recycled Aggregate and Powder Both from Clay Brick Waste. *Buildings* **2021**, *11*, 119. [CrossRef]
27. Zheng, L.; Ge, Z.; Yao, Z.; Gao, Z. Mechanical Properties of Mortar with Recycled Clay-Brick-Powder. In Proceedings of the ICCTP 2011: Towards Sustainable Transportation Systems. In Proceedings of the 11th International Conference of Chinese Transportation Professionals, Nanjing, China, 14–17 August 2011.
28. Liu, Q.; Li, B.; Xiao, J.; Singh, A. Utilization Potential of Aerated Concrete Block Powder and Clay Brick Powder from C&D Waste. *Constr. Build. Mater.* **2020**, *238*, 117721. [CrossRef]
29. Yoon, Y.S.; Yoo, D.Y. Influence of Steel Fibers and Fiber-Reinforced Polymers on the Impact Resistance of One-Way Concrete Slabs. *J. Compos. Mater.* **2014**, *48*, 695–706. [CrossRef]
30. Mohtasham Moein, M.; Mousavi, S.Y.; Madandoust, R.; Naser Saeid, H.N.S. The Impact Resistance of Steel Fiber Reinforcement Concrete under Different Curing Conditions: Experimental and Statistical Analysis. *J. Civil. Environ. Eng.* **2019**, *49*, 109–121. [CrossRef]
31. Murali, G.; Ramprasad, K. A Feasibility of Enhancing the Impact Strength of Novel Layered Two Stage Fibrous Concrete Slabs. *Eng. Struct.* **2018**, *175*, 41–49. [CrossRef]
32. Mohtasham Moein, M.; Saradar, A.; Rahmati, K.; Hatami Shirkouh, A.; Sadrinejad, I.; Aramali, V.; Karakouzian, M. Investigation of Impact Resistance of High-Strength Portland Cement Concrete Containing Steel Fibers. *Materials* **2022**, *15*, 7157. [CrossRef]
33. Al-Jabri, K.S.; Hago, A.W.; Tavakoli, D.; Waris, M.B.; Hassan, H.F.; Mohamedzein, Y. Investigating Thermal Cracking in Mass Concrete of a Bridge Abutment: Field Measurements and Numerical Modelling. *Aust. J. Civil. Eng.* **2022**, *22*, 146–162. [CrossRef]
34. Moein, M.M.; Saradar, A.; Rahmati, K.; Rezakhani, Y.; Ashkan, S.A.; Karakouzian, M. Reliability Analysis and Experimental Investigation of Impact Resistance of Concrete Reinforced with Polyolefin Fiber in Different Shapes, Lengths, and Doses. *J. Build. Eng.* **2023**, *69*, 106262. [CrossRef]
35. Al-Tayeb, M.M.; Al Daoor, I.; Wafi, S.R.; Tayeh, B. Ultimate Failure Resistance of Concrete with Partial Replacements of Sand by Polycarbonate Plastic Waste Under Impact Load. *Civil. Environ. Res.* **2020**, *12*, 42–49. [CrossRef]
36. Akçaözoğlu, S.; Atiş, C.D.; Akçaözoğlu, K. An Investigation on the Use of Shredded Waste PET Bottles as Aggregate in Lightweight Concrete. *Waste Manag.* **2010**, *30*, 285–290. [CrossRef] [PubMed]
37. Sharma, A.P.; Khan, S.H.; Velmurugan, R. Effect of through Thickness Separation of Fiber Orientation on Low Velocity Impact Response of Thin Composite Laminates. *Heliyon* **2019**, *5*, e02706. [CrossRef]
38. Abid, S.R.; Abdul-Hussein, M.L.; Ayoob, N.S.; Ali, S.H.; Kadhum, A.L. Repeated Drop-Weight Impact Tests on Self-Compacting Concrete Reinforced with Micro-Steel Fiber. *Heliyon* **2020**, *6*, e03198. [CrossRef] [PubMed]
39. Abid, S.R.; Shamkhi, M.S.; Mahdi, N.S.; Daek, Y.H. Hydro-Abrasive Resistance of Engineered Cementitious Composites with PP and PVA Fibers. *Constr. Build. Mater.* **2018**, *187*, 168–177. [CrossRef]
40. Rahmati, K.; Saradar, A.; Mohtasham Moein, M.; Sardrinejad, I.; Bristow, J.; Yavari, A.; Karakouzian, M. Evaluation of Engineered Cementitious Composites (ECC) Containing Polyvinyl Alcohol (PVA) Fibers under Compressive, Direct Tensile, and Drop-Weight Test. *Multiscale Multidiscip. Model. Exp. Des.* **2022**, *6*, 147–164. [CrossRef]
41. Abid, S.R.; Abdul Hussein, M.L.; Ali, S.H.; Kazem, A.F. Suggested Modified Testing Techniques to the ACI 544-R Repeated Drop-Weight Impact Test. *Constr. Build. Mater.* **2020**, *244*, 118321. [CrossRef]
42. Song, P.S. Statistical Analysis of Impact Strength and Strength Reliability of Steel—Polypropylene Hybrid Fiber-Reinforced Concrete. *Constr. Build. Mater.* **2005**, *19*, 1–9. [CrossRef]
43. Rahmani, T.; Kiani, B.; Shekarchi, M.; Safari, A. Statistical and Experimental Analysis on the Behavior of Fiber Reinforced Concretes Subjected to Drop Weight Test. *Constr. Build. Mater.* **2012**, *37*, 360–369. [CrossRef]
44. Zhu, P.; Mao, X.; Qu, W.; Li, Z.; Ma, Z.J. Investigation of Using Recycled Powder from Waste of Clay Bricks and Cement Solids in Reactive Powder Concrete. *Constr. Build. Mater.* **2016**, *113*, 246–254. [CrossRef]
45. Likes, L.; Markandeya, A.; Haider, M.M.; Bollinger, D.; McCloy, J.S.; Nassiri, S. Recycled Concrete and Brick Powders as Supplements to Portland Cement for More Sustainable Concrete. *J. Clean. Prod.* **2022**, *364*, 132651. [CrossRef]
46. Liu, S.; Dai, R.; Cao, K.; Gao, Z. The Role of Sintered Clay Brick Powder during the Hydration Process of Cement Pastes. *Iran. J. Sci. Technol.-Trans. Civil. Eng.* **2017**, *41*. [CrossRef]
47. Kim, J.; Lee, D.; Sičáková, A.; Kim, N. Utilization of Different Forms of Demolished Clay Brick and Granite Wastes for Better Performance in Cement Composites. *Buildings* **2023**, *13*, 159–165. [CrossRef]
48. Letelier, V.; Tarela, E.; Moriconi, G. Mechanical Properties of Concretes with Recycled Aggregates and Waste Brick Powder as Cement Replacement. *Procedia Eng.* **2017**, *171*, 627–632. [CrossRef]
49. Nepomuceno, M.C.S.; Isidoro, R.A.S.; Catarino, J.P.G. Mechanical Performance Evaluation of Concrete Made with Recycled Ceramic Coarse Aggregates from Industrial Brick Waste. *Constr. Build. Mater.* **2018**, *165*, 284–294. [CrossRef]
50. Olofinnade, O.M.; Ede, A.N.; Ndambuki, J.M.; Bamigboye, G.O. Structural Properties of Concrete Containing Ground Waste Clay Brick Powder as Partial Substitute for Cement. *Mater. Sci. Forum* **2016**, *866*, 63–67. [CrossRef]

51. Xue, C.; Shen, A.; Guo, Y.; He, T. Utilization of Construction Waste Composite Powder Materials as Cementitious Materials in Small-Scale Prefabricated Concrete. *Adv. Mater. Sci. Eng.* **2016**, *2016*, 8947935. [CrossRef]
52. Mohtasham Moein, M.; Rahmati, K.; Mohtasham Moein, A.; Rigby, S.E.; Saradar, A.; Karakouzian, M. Utilizing Construction and Demolition Waste in Concrete as a Sustainable Cement Substitute: A Comprehensive Study on Behavior Under Short-Term Dynamic and Static Loads via Laboratory and Numerical Analysis. *J. Build. Eng.* **2024**, *97*, 110778. [CrossRef]
53. Moein, M.M.; Soliman, A. Predicting the Compressive Strength of Alkali-Activated Concrete Using Various Data Mining Methods. In Proceedings of the Canadian Society of Civil Engineering Annual Conference, Moncton, NB, Canada, 24–27 May 2023; pp. 317–326.
54. Saradar, A.; Nemati, P.; Paskiabi, A.S.; Moein, M.M.; Moez, H.; Vishki, E.H. Prediction of Mechanical Properties of Lightweight Basalt Fiber Reinforced Concrete Containing Silica Fume and Fly Ash: Experimental and Numerical Assessment. *J. Build. Eng.* **2020**, *32*, 101732. [CrossRef]
55. Tahmouresi, B.; Nemati, P.; Asadi, M.A.; Saradar, A.; Mohtasham Moein, M. Mechanical Strength and Microstructure of Engineered Cementitious Composites: A New Configuration for Direct Tensile Strength, Experimental and Numerical Analysis. *Constr. Build. Mater.* **2021**, *269*, 121361. [CrossRef]
56. al-Swaidani, A.M.; Khwies, W.T.; al-Baly, M.; Lala, T. Development of Multiple Linear Regression, Artificial Neural Networks and Fuzzy Logic Models to Predict the Efficiency Factor and Durability Indicator of Nano Natural Pozzolana as Cement Additive. *J. Build. Eng.* **2022**, *52*, 104475. [CrossRef]
57. Golafshani, E.M.; Behnood, A.; Arashpour, M. Predicting the Compressive Strength of Normal and High-Performance Concretes Using ANN and ANFIS Hybridized with Grey Wolf Optimizer. *Constr. Build. Mater.* **2020**, *232*, 117266. [CrossRef]
58. Liu, K.; Alam, M.S.; Zhu, J.; Zheng, J.; Chi, L. Prediction of Carbonation Depth for Recycled Aggregate Concrete Using ANN Hybridized with Swarm Intelligence Algorithms. *Constr. Build. Mater.* **2021**, *301*, 124382. [CrossRef]
59. Prasad, N.; Murali, G. Exploring the Impact Performance of Functionally-Graded Preplaced Aggregate Concrete Incorporating Steel and Polypropylene Fibres. *J. Build. Eng.* **2021**, *35*, 102077. [CrossRef]
60. Huang, X.Y.; Wu, K.Y.; Wang, S.; Lu, T.; Lu, Y.F.; Deng, W.C.; Li, H.M. Compressive Strength Prediction of Rubber Concrete Based on Artificial Neural Network Model with Hybrid Particle Swarm Optimization Algorithm. *Materials* **2022**, *15*, 3934. [CrossRef] [PubMed]
61. Kandiri, A.; Sartipi, F.; Kioumarsi, M. Predicting Compressive Strength of Concrete Containing Recycled Aggregate Using Modified Ann with Different Optimization Algorithms. *Appl. Sci.* **2021**, *11*, 485. [CrossRef]
62. Heidari, A.; Hashempour, M.; Tavakoli, D. Using of Backpropagation Neural Network in Estimation of Compressive Strength of Waste Concrete. *J. Soft Comput. Civil. Eng.* **2017**, *1*, 48040. [CrossRef]
63. Srinivas, M.; Sucharitha, G.; Matta, A. *Machine Learning Algorithms and Applications*; CRC Press: Boca Raton, FL, USA, 2021.
64. Mehrotra, K.; Mohan, C.; Ranka, S. *Elements of Artificial Neural Networks*; MIT Press: Cambridge, MA, USA, 2019.
65. Mohtasham Moein, M.; Saradar, A.; Rahmati, K.; Ghasemzadeh Mousavinejad, S.H.; Bristow, J.; Aramali, V.; Karakouzian, M. Predictive Models for Concrete Properties Using Machine Learning and Deep Learning Approaches: A Review. *J. Build. Eng.* **2023**, *63*, 105444. [CrossRef]
66. Zadeh, L.A. Fuzzy Sets. *Inf. Control* **1965**, *8*, 338–353. [CrossRef]
67. Mohd Adnan, M.R.H.; Sarkheyli, A.; Mohd Zain, A.; Haron, H. Fuzzy Logic for Modeling Machining Process: A Review. *Artif. Intell. Rev.* **2015**, *43*, 345–379. [CrossRef]
68. Uplenchwar, K.B.; Kokate, R.S. Application of Fuzzy Logic: A Review. *Int. Res. J. Eng. Technol.* **2020**, *7*, 2097–2100.
69. Serrano-Guerrero, J.; Romero, F.P.; Olivas, J.A. Fuzzy Logic Applied to Opinion Mining: A Review. *Knowl. Based Syst.* **2021**, *222*, 107018. [CrossRef]
70. Soltanifar, M.; Sharafi, H.; Hosseinzadeh Lotfi, F.; Pedrycz, W.; Allahviranloo, T. Introduction to Fuzzy Logic. In *Studies in Systems, Decision and Control*; MIT Press: Cambridge, MA, USA, 2023; Volume 471.
71. Zadeh, L.A. Is There a Need for Fuzzy Logic? *Inf. Sci.* **2008**, *178*, 2751–2779. [CrossRef]
72. Abbas, Y.M.; Iqbal Khan, M. Prediction of Compressive Stress–Strain Behavior of Hybrid Steel–Polyvinyl-Alcohol Fiber Reinforced Concrete Response by Fuzzy-Logic Approach. *Constr. Build. Mater.* **2023**, *379*, 131212. [CrossRef]
73. Güler, K.; Demir, F.; Pakdamar, F. Stress-Strain Modelling of High Strength Concrete by Fuzzy Logic Approach. *Constr. Build. Mater.* **2012**, *37*, 680–684. [CrossRef]
74. Weibull, W. A Statistical Theory of the Strength of Materials. Generalstabens Litografiska Anstalts Förlag, Stockholm. *Gen. Litografiska Anst. Förlag* **1939**, *151*, 189–206.
75. Jung, C.; Schindler, D. Wind Speed Distribution Selection—A Review of Recent Development and Progress. *Renew. Sustain. Energy Rev.* **2019**, *114*, 109290. [CrossRef]
76. Wais, P. Two and Three-Parameter Weibull Distribution in Available Wind Power Analysis. *Renew. Energy* **2017**, *103*, 15–29. [CrossRef]
77. Gerhards, C.; Schramm, M.; Schmid, A. Use of the Weibull Distribution Function for Describing Cleaning Kinetics of High Pressure Water Jets in Food Industry. *J. Food Eng.* **2019**, *253*, 21–26. [CrossRef]
78. Idiapho, O.K.; Odinikuku, W.E.; Akusu, O.M. Reliability Assessment of a Cement Industry by Application of Weibull Method. *J. Eng. Res. Rep.* **2019**, *7*, 1–11. [CrossRef]

79. Shah, K.; Khurshid, H.; Haq, I.U.; Ali Shah, S.; Ali, Z. Forecasting Machine Failure Using DMG and Weibull Analysis in an Automotive Industry: A Case Study. *Mehran Univ. Res. J. Eng. Technol.* **2021**, *40*, 435–442. [CrossRef]
80. Abirami, T.; Loganaganandan, M.; Murali, G.; Fediuk, R.; Vickhram Sreekrishna, R.; Vignesh, T.; Januppriya, G.; Karthikeyan, K. Experimental Research on Impact Response of Novel Steel Fibrous Concretes under Falling Mass Impact. *Constr. Build. Mater.* **2019**, *222*, 447–457. [CrossRef]
81. Swaminathan, P.; Karthikeyan, K.; Subbaram, S.R.; Sudharsan, J.S.; Abid, S.R.; Murali, G.; Vatin, N.I. Experimental and Statistical Investigation to Evaluate Impact Strength Variability and Reliability of Preplaced Aggregate Concrete Containing Crumped Rubber and Fibres. *Materials* **2022**, *15*, 5156. [CrossRef] [PubMed]
82. Murali, G.; Asrani, N.P.; Ramkumar, V.R.; Siva, A.; Haridharan, M.K. Impact Resistance and Strength Reliability of Novel Two-Stage Fibre-Reinforced Concrete. *Arab. J. Sci. Eng.* **2019**, *44*, 4477–4490. [CrossRef]
83. *ASTM C33/C33M-16*; Standard Specification for Concrete Aggregates. ASTM International: West Conshohocken, PA, USA, 2016.
84. Ma, Z.; Li, W.; Wu, H.; Cao, C. Chloride Permeability of Concrete Mixed with Activity Recycled Powder Obtained from C&D Waste. *Constr. Build. Mater.* **2019**, *199*, 652–663. [CrossRef]
85. Xiao, J.; Ma, Z.; Sui, T.; Akbarnezhad, A.; Duan, Z. Mechanical Properties of Concrete Mixed with Recycled Powder Produced from Construction and Demolition Waste. *J. Clean. Prod.* **2018**, *188*, 720–731. [CrossRef]
86. Ahmed, J.K.; Atmaca, N.; Khoshnaw, G.J. Building a Sustainable Future: An Experimental Study on Recycled Brick Waste Powder in Engineered Geopolymer Composites. *Case Stud. Constr. Mater.* **2024**, *20*, e02863. [CrossRef]
87. *ASTM C618*; Standard Specification for Coal Fly Ash and Raw or Calcinated Natural Pozzolan for Use in Concrete. Annual Book of ASTM Standards; ASTM International: West Conshohocken, PA, USA, 2005; Volume 1479.
88. *ASTM C192/C192M-19*; Standard Practice for Making and Curing Concrete Test Specimens in the Laboratory. ASTM International: West Conshohocken, PA, USA, 2019.
89. Ge, Z.; Gao, Z.; Sun, R.; Zheng, L. Mix Design of Concrete with Recycled Clay-Brick-Powder Using the Orthogonal Design Method. *Constr. Build. Mater.* **2012**, *31*, 289–293. [CrossRef]
90. *BS EN 12390-3:2019*; Testing Hardened Concrete Part 3: Compressive Strength of Test Specimens. British Standards Institution; BSI Standards Publication: London, UK, 2019.
91. *ASTM C348-21*; Standard Test Method for Flexural Strength of Hydraulic-Cement Mortars. ASTM International: West Conshohocken, PA, USA, 2021; Volume 4.
92. *ASTM C 496M-02 C496-96*; Standard Test Method for Splitting Tensile Strength of Cylindrical Concrete. ASTM International: West Conshohocken, PA, USA, 2002; Volume 4.
93. ACI Committee 544. State-of-the-Art Report on Fiber Reinforced Concrete. ACI Committee 544 Report 544,1R-96. In *ACI Committee 544*; American Concrete Institute: Detroit, MI, USA, 1996.
94. Figueiredo, M.; Gomide, F.; Rocha, A.; Yager, R. Comparison of Yager's Level Set Method for Fuzzy Logic Control with Mamdani's and Larsen's Methods. *IEEE Trans. Fuzzy Syst.* **1993**, *1*, 156–159. [CrossRef]
95. Blej, M.; Azizi, M. Comparison of Mamdani-Type and Sugeno-Type Fuzzy Inference Systems for Fuzzy Real Time Scheduling. *Int. J. Appl. Eng. Res.* **2016**, *11*.
96. Mada, G.S.; Dethan, N.K.F.; Maharani, A.E.S.H. The Defuzzification Methods Comparison of Mamdani Fuzzy Inference System in Predicting Tofu Production. *J. Varian* **2022**, *5*, 11071–11075. [CrossRef]
97. Santhosh, A.M.; Thomas, A. Experimental Studies on Brick Powder Replaced Concrete Exposed to Elevated Temperature. In *Lecture Notes in Civil Engineering*; Springer: Berlin/Heidelberg, Germany, 2020; Volume 46.
98. Sallı Bideci, Ö.; Bideci, A.; Ashour, A. Utilization of Recycled Brick Powder as Supplementary Cementitious Materials—A Comprehensive Review. *Materials* **2024**, *17*, 637. [CrossRef] [PubMed]
99. Bertelsen, I.M.G.; Kahr, S.A.; Kunther, W.; Ottosen, L.M. Clay Brick Powder as Partial Cement Replacement. In *RILEM Bookseries*; Springer: Berlin/Heidelberg, Germany, 2023; Volume 44.
100. Mangngi, P.; Tjaronge, M.W.; Caronge, M.A. Durability Assessment of Concrete Containing Recycled Coarse Refractory Brick Aggregate. *Innov. Infrastruct. Solut.* **2024**, *9*, 144. [CrossRef]
101. Kim, Y.J. Quality Properties of Self-Consolidating Concrete Mixed with Waste Concrete Powder. *Constr. Build. Mater.* **2017**, *135*, 177–185. [CrossRef]
102. Rani, M.U.; Jenifer, J.M. Mechanical Properties of Concrete with Partial Replacement of Portland Cement by Clay Brick Powder. *IJERT—Int. J. Eng. Res. Technol.* **2016**, *5*, 2181–2278.
103. Lin, K.L.; Wu, H.H.; Shie, J.L.; Hwang, C.L. An Cheng Recycling Waste Brick from Construction and Demolition of Buildings as Pozzolanic Materials. *Waste Manag. Res.* **2010**, *28*, 653–659. [CrossRef]
104. Karatas, M.; Acikgenc, M.; Ulucan, Z.C. Effects of Elazig Region Waste Brick and Limestone Powder on Engineering Properties of Self-Compacting Mortar. *Pamukkale Univ. J. Eng. Sci.* **2013**, *19*, 249–255. [CrossRef]
105. Heidari, A.; Hasanpour, B. Effects of Waste Bricks Powder of Gachsaran Company as a Pozzolanic Material in Concrete. *Asian J. Civil. Eng.* **2013**, *14*, 755–763.
106. Xue, C.Z.; Shen, A.Q.; Chang, Y.T.; Liang, D. The Study of the Construction Waste Brick Powder's Activity. *Adv. Mat. Res.* **2014**, *1079–1080*, 309–311. [CrossRef]

107. Ayaz Khan, M.N.; Liaqat, N.; Ahmed, I.; Basit, A.; Umar, M.; Khan, M.A. Effect of Brick Dust on Strength and Workability of Concrete. In Proceedings of the IOP Conference Series: Materials Science and Engineering, Melbourne, Australia, 15–16 September 2018; Volume 414.
108. Ortega, J.M.; Letelier, V.; Solas, C.; Moriconi, G.; Climent, M.Á.; Sánchez, I. Long-Term Effects of Waste Brick Powder Addition in the Microstructure and Service Properties of Mortars. *Constr. Build. Mater.* **2018**, *182*, 691–702. [CrossRef]
109. Beshkari, M.; Amani, B.; Rahmati, K.; Mohtasham Moein, M.; Saradar, A.; Karakouzian, M. Synergistic Effects of Pozzolan and Carbon Fibers on the Performance of Self-Consolidating Concrete under Plastic Shrinkage and Dynamic Loading. *Innov. Infrastruct. Solut.* **2024**, *9*, 160. [CrossRef]
110. Ismail, M.K.; Hassan, A.A.A.; Lachemi, M. Performance of Self-Consolidating Engineered Cementitious Composite under Drop-Weight Impact Loading. *J. Mater. Civil. Eng.* **2019**, *31*, 04018400. [CrossRef]
111. Gupta, T.; Sharma, R.K.; Chaudhary, S. Impact Resistance of Concrete Containing Waste Rubber Fiber and Silica Fume. *Int. J. Impact Eng.* **2015**, *83*, 76–87. [CrossRef]
112. Nataraja, M.C.; Dhang, N.; Gupta, A.P. Statistical Variations in Impact Resistance of Steel Fiber-Reinforced Concrete Subjected to Drop Weight Test. *Cem. Concr. Res.* **1999**, *29*, 989–995. [CrossRef]
113. Song, P.S.; Wu, J.C.; Hwang, S.; Sheu, B.C. Assessment of Statistical Variations in Impact Resistance of High-Strength Concrete and High-Strength Steel Fiber-Reinforced Concrete. *Cem. Concr. Res.* **2005**, *35*, 393–399. [CrossRef]
114. Chen, X.Y.; Ding, Y.N.; Azevedo, C. Combined Effect of Steel Fibres and Steel Rebars on Impact Resistance of High Performance Concrete. *J. Cent. South Univ.* **2011**, *18*, 1677–1684. [CrossRef]
115. Murali, G.; Abid, S.R.; Mugahed Amran, Y.H.; Abdelgader, H.S.; Fediuk, R.; Susrutha, A.; Poonguzhali, K. Impact Performance of Novel Multi-Layered Prepacked Aggregate Fibrous Composites under Compression and Bending. *Structures* **2020**, *28*, 1502–1515. [CrossRef]
116. Meng, J.; Xu, Z.; Liu, Z.; Chen, S.; Wang, C.; Zhao, B.; Zhou, A. Experimental Study on the Mechanics and Impact Resistance of Multiphase Lightweight Aggregate Concrete. *Sustainability* **2022**, *14*, 9606. [CrossRef]

Disclaimer/Publisher's Note: The statements, opinions and data contained in all publications are solely those of the individual author(s) and contributor(s) and not of MDPI and/or the editor(s). MDPI and/or the editor(s) disclaim responsibility for any injury to people or property resulting from any ideas, methods, instructions or products referred to in the content.